Master of Medical Science in Virology

Research Project Topic:

Characterization of HIV-1 Env found in virus reservoirs in lymph nodes and peripheral blood

Name: Siyamthemba Dlamini

Student Number: 216054747

Supervisor: Prof. Jaclyn Mann

School of Laboratory Medicine and Medical Sciences

College of Health Sciences

University of KwaZulu-Natal

2026

Table of Contents

List of Figures

List of Tables

Preface

This project represents original work done by the author and others whose contribution has been acknowledged in the text. All experimental work mentioned in this dissertation was accomplished in the P2+ Laboratory and Hasso Plattner Research Laboratory at the HIV Pathogenesis Programme, which is located in the Doris Duke Medical Research Institute, Nelson R. Mandela School of Medicine, University of Kwa-Zulu Natal, Durban, South Africa, from March 2024 to November 2025, under the supervision of Professor Jaclyn Mann.

Student Name: **Siyamthemba Oswald Dlamini**

Student signature: _____ Date: **29 January 2026**

Supervisor Name: **Prof Jaclyn Mann**

Supervisor signature: Date: **2 February 2026**

Declaration

I, **Siyamthemba Oswald Dlamini**, declare that:

(i) The research reported in this study, except otherwise indicated, is my original work.

(ii) This study has not been submitted for any degree or examination at any other university.

(iii) This study does not contain other person's data, pictures, graphs, or other information, unless specifically acknowledged as being sourced from other persons.

(iv) This dissertation does not contain other person's writing, unless specifically acknowledged as being sourced from other researchers. Where other written sources have been quoted, then:

a) Their words have been re-written, but the general information attributed to them has been referenced.

b) Where their exact words have been used, their writing has been placed inside quotation marks and referenced.

(v) This dissertation does not contain text, graphics or tables copied and pasted from the internet unless specifically acknowledged, and the source being detailed in the dissertation and in the references section.

Acknowledgements

I would like to give special thanks to:

- My family for their unwavering support and love throughout my degree.
- My supervisor, Professor Jaclyn Mann, whose mentorship made this entire journey possible. Her guidance and encouragement not only shaped this project but were also pivotal to my success during my Masters. I am truly and forever grateful.
- The amazing staff at HIV Pathogenesis Programme.
- The Sub-Saharan African Network for TB/HIV Research Excellence (SANTHE), Poliomyelitis Research Foundation (PRF) and the HIV Pathogenesis Programme (HPP) for the financial support throughout this degree.
- My colleagues who made the long days enjoyable and most importantly memorable.
- My closest friends that have shared this journey with me and always reminded me that the goal was always within sight.

Abbreviations

ADCC - antibody-dependent cellular cytotoxicity

AIDS - acquired immunodeficiency syndrome

AMP - Antibody Mediated Prevention

bNAbs - broadly neutralizing antibodies

BREC - Biomedical Research Ethics Committee

cDNA - complementary DNA

CMV - Cytomegalovirus

CNS - central nervous system

cTfh - T follicular helper cells

CTLs - cytotoxic T lymphocytes

dCA - didehydro-cortistatin A

DMEM - Dulbecco's Modified Eagle Medium

Env - envelope glycoprotein

FBS - Fetal bovine serum

FDCs - follicular dendritic cells

GALT - gut-associated lymphoid tissue

GI - gastrointestinal

HEPES - 4-(2-hydroxyethyl)-1-piperazineethanesulfonic acid

HPP - HIV pathogenesis programme

IC50 - 50% inhibitory concentration

IQR - Inter-quartile range

LNs - Lymph nodes

LN - Lymph node

LTR - Long terminal repeat

MHC - Major histocompatibility complex

mTOR - mechanistic target of rapamycin

MPER - membrane-proximal external region

NK - natural killer cells

PBMCs – peripheral blood mononuclear cells

PCR - polymerase chain reaction

PEI - polyethylenimine

PFA - paraformaldehyde

PL - plasma

PLWH - people were living with HIV

PNGSs - potential N-linked glycosylation sites

TCID - Tissue Culture Infectious Dose

TF - transmitted/founder

TLR - Toll-like receptor

Dedication

I dedicate this work to my family; at the core of what I do is you. This passion, this drive only exists because you inspire me to, and I will forever be grateful for the role you have played in my life. I love you guys so much.

Abstract

The persistence of latent, replication-competent viral reservoirs in people living with HIV (PLWH) on suppressive antiretroviral therapy (ART) remains the principal barrier to a cure. Broadly neutralizing antibodies (bNAbs), which target Env, represent a promising immunotherapeutic strategy to clear infected cells and block viral rebound. A key unresolved question is whether the viral variants that populate these anatomical reservoirs, particularly within lymphoid tissues and peripheral blood, harbour genetic differences that could confer altered sensitivity to bNAbs. Understanding this is important for the design of effective antibody-based interventions, as mutations in variants persisting in the reservoir could allow reservoir viruses to evade bNAb therapy. To address this, we conducted a comparative analysis of HIV-1 env sequences and bNAb neutralization sensitivity for viral variants derived from pre-ART plasma (PL), and post-ART peripheral blood mononuclear cells (PBMCs) and lymph node (LN) reservoirs in individuals living with HIV-1 subtype C.

The study cohort comprised 11 adults from Durban, South Africa, on suppressive ART. Bulk *env* sequences were generated from pre-therapy plasma, and from PBMC and LN mononuclear cells sampled after one year of therapy and next generation sequencing was performed on *env* amplicons from pre-therapy plasma. Sequences were assessed for unique genetic differences in the reservoir variants. For a subset of six participants, selected to represent a range of genetic differences, functional recombinant Env viruses were generated for each compartment from bulk participant-derived *env* amplicons and a replication-competent *env*-deleted NL4-3 plasmid backbone. Infectious virus stocks were produced via transfection of *env* amplicons and plasmid backbone into HEK293T cells, followed by further passaging of stocks in CEM-derived GXR25 T cells. Neutralization sensitivity of viruses was determined using a standardized TZM-bl cell assay and a panel of nine clinically relevant bNAbs targeting major epitopes - the CD4-binding site (VRC01, VRC07-523LS, N6), the V3-glycan supersite (10-1074, PGT121), the V2-glycan apex (PGDM1400, CAP256-VRC26.25), the gp120-gp41 interface (PGT151), and the membrane-proximal external region (MPER) (10E8).

Phylogenetic analysis confirmed participant-specific clustering of sequences and excluded cross-contamination. Analysis of sequencing data revealed a median of 6 (inter-quartile range [IQR] 3–22.5) and 19 (IQR 7–49) amino acid differences between pre-therapy plasma sequences and LN and PBMC reservoirs, respectively. Notably, 63% of LN and 73% of PBMC

reservoir mutations were unique to the reservoir. However, only a median of 0 (LN) and 2 (PBMC) of these changes occurred at positions known to affect bNAb sensitivity.

Neutralization assays using viruses from six participants against nine bNAbs showed that no consistent pattern of increased or decreased sensitivity was observed in one compartment over another - sensitivity was highly variable and dependent on the participant, viral compartment, and specific bNAb. Overall, most viruses were sensitive to the CD4 binding site antibodies regardless of compartment (IC50 median = 0.11 µg/ml; IQR = 0.05 – 0.17). Similarly, all viruses, with the exception of one with markedly reduced sensitivity (20 µg/ml), were sensitive to the interface antibody (median = 0.1; IQR = 0.07 – 0.18). On the other hand, resistance to V2 and V3 antibodies was more common, and varied between compartments, with IC50s >10 ug/ml in 80% (CAP256), 13.3% (PGDM1400) 73.3% (PGT121), and 80% (10-1074) of the viruses. There were mixed results for the MPER antibody, where most of the viruses were sensitive to the MPER with the exception of two viruses.

These findings show that HIV-1 subtype C reservoir Env variants harbour genetic differences from pre-therapy plasma variants, but that this variation was seldom at sites reported to affect bNAb sensitivity and also did not result in consistent, compartment-specific differences in neutralization sensitivity to a broad panel of bNAbs. While clear genotype–phenotype associations were evident for some epitopes (notably the V3-glycan supersite), sequence data alone did not fully predict neutralization outcomes. The neutralization sensitivity results underscored the suitability of the CD4bs and interface as promising therapeutic targets for bNAb therapy and reinforced the rationale for combination bNAb regimens. Together, these results highlight the importance of integrating genetic and functional analyses when assessing reservoir susceptibility and provide data that may inform the rational design of combination bNAb strategies for subtype C infection.

Chapter 1 – Literature Review

1.1 Introduction to HIV-1

1.1.1 HIV epidemic

As of 2023, an estimated 39.9 million PLWH globally, including 38.6 million adults and 1.4 million children (WHO, 2023). Africa remains the most heavily affected region, with approximately 25.6 million PLWH, and Southern Africa alone accounts for an estimated 20.8 million of these cases [1]. The advent of ART has significantly improved the quality of life and survival of PLWH by transforming HIV into a manageable chronic condition [1]. However, it remains an imperfect solution due to various limitations [1]. Despite significant progress in controlling the HIV pandemic through the widespread use of ART, these treatments do not eliminate the virus, necessitating lifelong adherence [1]. Furthermore, long-term ART use is associated with an elevated risk of non-communicable diseases, including cardiovascular, metabolic, and neurological complications, creating a complex chronic disease management landscape [2]. Limited access to healthcare infrastructure remains a significant barrier to effective ART delivery, particularly in under-resourced regions such as sub-Saharan Africa, where many people live below the poverty line [1]. There is, therefore, an urgent need for durable, effective solutions aimed at either the complete eradication or long-term remission of HIV infection [1].

Although achieving a cure may seem ambitious, recent scientific advances have provided promising insights that are now guiding HIV vaccine and cure research [3]. Examples include long-term viral remission achieved in at least two individuals following allogeneic hematopoietic stem cell transplantation, sustained control observed in elite controllers (approximately 1% of PLWH), and post-treatment controllers, individuals who maintain viral suppression after early ART initiation and subsequent treatment interruption [4].

1.1.2 HIV genome and replication

HIV exists in two major types, HIV-1 and HIV-2. HIV-1 is further classified into four groups (M, N, O, and P), with Group M responsible for over 95% of global infections [5]. Both HIV-1 and HIV-2 belong to the Retroviridae family, and the genus *Lentivirus*, characterized by their long incubation periods and capacity for persistent infection [6]. The WHO international standard for HIV-1 RNA genome length is 8,926 nucleotides, with a guanine–cytosine (G+C) content of approximately 41% [7]. The coding region spans 8,606

nucleotides and encodes nine open reading frames (*gag*, *pol*, *vif*, *vpr*, *tat*, *rev*, *vpu*, *env*, and *nef*). The genome also includes a complete U5 region, part of the R region in the 5' long terminal repeat (LTR) (5'-LTR), and a small U3 region from the 3'-LTR [7]. HIV targets the host immune system by infecting CD4+ T cells. Viral entry is mediated by the Env, which facilitates the delivery of the viral genome into host cells [8]. The gp120 subunit of Env binds to the CD4 receptor and co-receptors (CCR5 or CXCR4) on the host cell surface. This interaction triggers conformational changes in gp120, exposing gp41, which then mediates the fusion of viral and host cell membranes, allowing viral entry [6].

Following membrane fusion, the viral core is released into the cytoplasm of the host cell where reverse transcription of the single-stranded RNA genome into double-stranded DNA occurs, catalysed by the viral reverse transcriptase enzyme [9]. This newly formed viral DNA is then transported into the nucleus as part of a pre-integration complex and is integrated into the host cell's chromosomal DNA by the viral integrase enzyme, forming a provirus [10]. Upon cellular activation, the integrated proviral DNA is transcribed by the host cell's RNA polymerase II, generating new viral genomic RNA and spliced messenger RNAs (mRNAs) [11]. These mRNAs are exported to the cytoplasm and translated to produce viral structural proteins (Gag, Pol) and envelope Env, as well as accessory proteins [12]. The full-length genomic RNA, along with viral proteins, assembles at the host cell membrane where the immature virion buds from the cell [13]. Finally, maturation into an infectious virion is completed through proteolytic cleavage of the Gag and Gag-Pol polyproteins by the viral protease, leading to the rearrangement of the core into its mature, conical structure [14].

1.1.3 HIV pathogenesis overview

Despite encoding only 15 mature proteins, HIV demonstrates remarkable evolutionary success by persistently infecting hosts and effectively evading both innate and adaptive immune responses [6].

HIV infection is marked by a gradual decline in CD4+ T cell counts. When levels fall below 200 cells/µL, the individual is considered to have progressed to acquired immunodeficiency syndrome (AIDS) [8]. Following transmission, HIV primarily targets CD4+ T lymphocytes, dendritic cells, and macrophages by binding to the CD4 receptor and a co-receptor (CCR5 or CXCR4) on the cell surface [15]. The initial acute phase of infection is

characterized by rapid viral replication and a sharp, transient decline in peripheral CD4+ T cell counts, accompanied by a spike in plasma viremia [16]. During this phase, the host mounts a robust innate immune response, including the production of type I interferons and the activation of natural killer (NK) cells, followed by the development of HIV-specific adaptive immunity, notably cytotoxic T lymphocytes (CTLs) and humoral responses [17]. These immune responses, particularly the CTL response, partially control viral replication, leading to a set-point viremia and a clinically latent, chronic phase that can last for years [18].

HIV employs multiple strategies to evade these defences, including high mutation rates and rapid replication that generate escape variants from CTL recognition, the shielding of conserved envelope regions with glycans to neutralize antibody binding, and the downregulation of MHC (Major histocompatibility complex) class I molecules on infected cells to hide from immune surveillance [19]. The chronic, high-level immune activation driven by persistent viral replication and microbial translocation from a damaged gut mucosa ultimately leads to the progressive exhaustion of the immune system and the gradual decline in CD4+ T cell counts [20]. When CD4+ T cell levels fall below 200 cells/μL, the individual is considered to have progressed to AIDS, characterized by the onset of opportunistic infections and malignancies [21].

1.2 Virus reservoirs in HIV infection.

1.2.1 HIV latency and the role of viral reservoirs in HIV persistence

HIV latency represents one of the primary obstacles to achieving either a sterilising or functional cure for HIV-1 infection [22]. Latency is established when the virus integrates its genome into the host cell DNA and enters a transcriptionally silent state, thereby evading both immune recognition and the cytopathic effects of active replication [22]. Crucially, this latent state is established rapidly following initial infection, often within days, which explains why eradication remains elusive even when ART is initiated during acute infection [23].

Although ART is highly effective in suppressing viral replication and reducing plasma viremia to undetectable levels, it cannot eliminate latent reservoirs [24]. Several

mechanisms enable this persistence, including epigenetic modifications of the viral promoter, limited access to necessary transcription factors, and the long-lived nature of memory CD4+ T cells that harbour proviral DNA [25]. Collectively, these mechanisms create a formidable barrier to both immune-mediated clearance and therapeutic intervention.

Traditionally, latency has been conceptualised as complete transcriptional silence [25]. However, increasing evidence challenges this definition, suggesting that some reservoir cells exhibit low-level or intermittent transcriptional activity further complicating eradication strategies such as "shock and kill," which rely on uniform reactivation of latent proviruses [25].

The nature and distribution of reservoirs further complicate efforts to achieve a cure (Figure 1.1). While resting memory CD4+ T cells remain the most studied reservoir, additional cell types, including macrophages and follicular dendritic cells (FDCs) may also play a role in maintaining persistence [26]. Moreover, viral reservoirs are not restricted to peripheral blood but are widely distributed across tissues, including lymph nodes (LNs), gut-associated lymphoid tissue (GALT), and the central nervous system, each providing distinct microenvironments that limit both drug penetration and immune surveillance [27]. Nevertheless, much of what is known about reservoirs comes from studies of PBMCs, which may underestimate the true scope and heterogeneity of persistence due to the practical and ethical challenges of tissue sampling [26].

There is also ongoing debate regarding the mechanisms that sustain reservoirs over time. While some evidence points to clonal proliferation of latently infected cells as a major contributor, other studies highlight the possibility of residual viral replication in anatomical sanctuaries where ART penetration is suboptimal [28]. Clarifying the importance of these mechanisms is essential, as it will shape the design of cure strategies and whether they should primarily target cellular proliferation or focus on intensifying ART to fully suppress replication [28].

HIV latency and the persistence of viral reservoirs remain the principal barriers to a cure [26]. Despite significant progress in elucidating their molecular and cellular mechanisms, major gaps remain regarding tissue-specific reservoir dynamics, the spectrum of latency,

and the mechanisms sustaining persistence [26]. Addressing these uncertainties is critical for the development of effective and durable cure strategies.

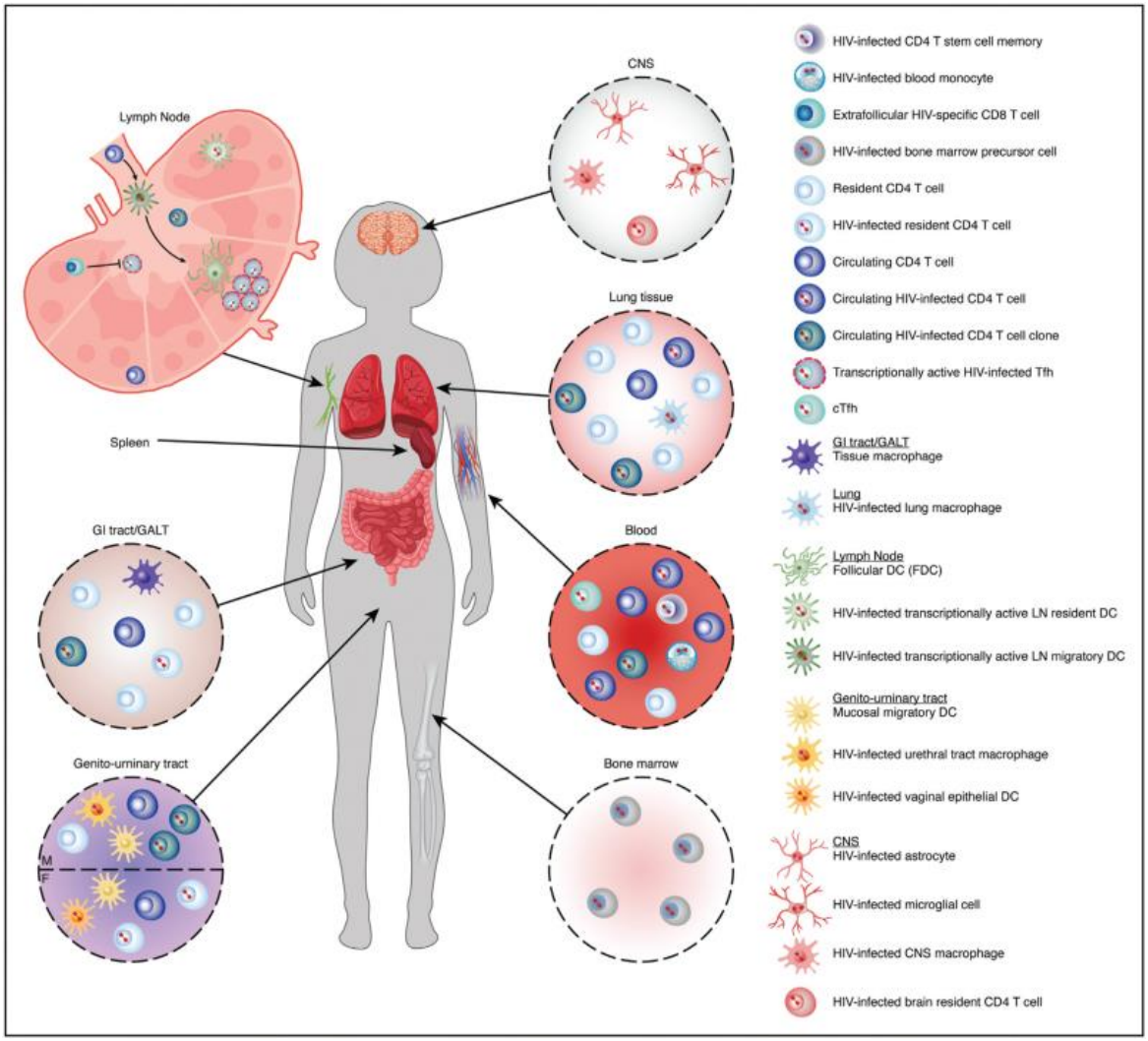

Figure 1.1 Potential HIV tissue reservoirs in the body. The figure illustrates the intricate nature of the HIV reservoir during antiretroviral therapy, highlighting its diverse cellular makeup, widespread anatomical distribution, and varying transcriptional states. It maps key reservoir sites across the body, including the blood, lymphoid organs (spleen, LNs, and GALT), bone marrow, lungs, genitourinary tract, and central nervous system (CNS). Different cell types within these sites are represented, with a distinction made between cells harbouring latent, integrated HIV DNA and those that are transcriptionally active (indicated by dashed red lines). Specific annotations include circulating T follicular helper cells (cTfh), the gastrointestinal (GI) tract, and separate designations for the male (M) and female (F) genital tracts. This diagram was sourced from Banga and Perreau (2024) (Creative commons license: CC BY-NC-ND 4.0) [29].

1.2.2 The cell biology of the HIV-1 latent reservoir

While latent HIV infection has been detected in various circulating blood cells [30], the CD4+ T lymphocyte compartment, particularly long-lived resting memory subsets, is widely recognized as the principal cellular reservoir, with integrated provirus exhibiting minimal decay over time [22]. However, the complexity of viral persistence extends beyond a single cell type [26]. A diverse range of cells can harbour latent or inducible virus, including monocyte-derived macrophages and microglia in tissues, which are resistant to cytopathic effects and can reseed infection [26]. These include but are not limited to FDCs in lymphoid tissues, which trap infectious virions extracellularly and, more controversially, certain hematopoietic progenitor cells and astrocytes [31-33].

This cellular heterogeneity highlights that the reservoir is not monolithic. Critically, the persistence and dynamics of these infected cells are fundamentally shaped by their microenvironment [34]. Therefore, the anatomical sanctuaries that shelter them, particularly the structured lymphoid tissues like LNs and gut-associated lymphoid tissue (GALT), are of paramount importance [34]. These sites provide protective niches that foster latency, limit immune surveillance and drug penetration, and facilitate low-level viral replication, making them central to understanding reservoir persistence and the challenges of a cure [34].

1.2.3 Importance of LNs and their role viral reservoir persistence.

Lymphoid tissues, particularly LNs, are increasingly recognised as critical sites for the persistence of HIV reservoirs during ART [29]. These secondary lymphoid organs provide both a structural and immunological niche that facilitates the survival of latently infected cells, thereby posing a major obstacle to viral eradication [35].

One of the defining features of LNs is their highly compartmentalised architecture, which enables close interactions between T cells, B cells, dendritic cells, and FDCs [36]. This microenvironment not only supports effective immune surveillance but also inadvertently promotes the maintenance of viral reservoirs [37]. Notably, HIV DNA and replication-

competent virus have consistently been detected within LN tissues of PLWH despite sustained viral suppression by ART [29]. These findings underscore the fact that systemic viral control in peripheral blood does not necessarily reflect the control of infection within tissue reservoirs.

A central mechanism underlying this persistence is the sequestration of the virus on the surface of FDCs [36]. Rather than being productively infected themselves, FDCs trap HIV in immune complexes that remain infectious for extended periods [29]. Such immune complexes can subsequently transfer the virus to CD4+ T cells, even in the context of ART, thereby sustaining the reservoir [38]. Importantly, the replication-competent virus found in LNs has been shown to be genetically diverse, highlighting ongoing viral evolution and suggesting that lymphoid tissues may act as sites of residual viral replication [39]. This remains a matter of debate, with some evidence supporting low-level ongoing replication in lymphoid tissues, while other studies argue that persistence is predominantly driven by clonal proliferation of infected CD4+ T cells [40].

The spatial organisation of LNs further contributes to incomplete ART penetration [41]. Studies have shown that certain anatomical compartments within LNs exhibit suboptimal drug concentrations, creating pharmacological sanctuaries that allow the persistence of viral reservoirs [41]. This pharmacological limitation, coupled with the immune-privileged nature of B-cell follicles where cytotoxic CD8+ T cells have restricted access, establishes an environment highly conducive to viral persistence [29]. The inability of effector immune cells to efficiently eliminate infected CD4+ T cells within these niches represents a fundamental barrier to eradication strategies.

Critically, LN reservoirs have also been implicated in viral rebound following treatment interruption [29]. When ART is discontinued, replication-competent viruses harboured within LNs rapidly reseed peripheral blood, leading to systemic viremia [29]. A study using barcoded SIV in rhesus macaques to trace the origins of viral rebound identified secondary lymphoid tissues specifically the mesenteric LNs, inguinal LNs, and spleen as key sources of rebound-competent virus despite undetectable plasma viremia [42]. In contrast, a clinical study analysing rebound HIV in participants found no primary anatomical source, instead revealing a genetically heterogeneous reservoir [39]. These findings suggest that while LNs are clearly established as critical anatomical reservoirs,

human data indicate they are not necessarily the singular or dominant source of viral rebound, which likely arises from a widely dispersed reservoir of infected cells.

LNs serve as a major anatomical reservoir of HIV persistence by combining structural, immunological, and pharmacological factors that enable the long-term maintenance of latent infection [29]. While significant progress has been made in identifying the mechanisms that underpin this persistence, ongoing debates such as whether viral reservoirs are sustained by low-level replication versus clonal expansion illustrate the complexity of targeting LN reservoirs [29]. A deeper understanding of these dynamics will be essential for designing cure-focused strategies.

1.2.4 Population-specific determinants of HIV reservoir size

Most studies of HIV-1 persistence have focused on middle-aged men from high-income settings, typically infected with subtype B virus and initiating ART during chronic infection [34]. While such studies have provided important insights, their findings are not universally generalisable [34]. It is now well established that biological sex, age, HIV subtype, timing of ART initiation, and co-infections all influence the size, distribution, and activity of the latent reservoir [34].

Biological sex

In the absence of therapy, women generally present with lower plasma viral loads than men, particularly during early-stage infection, an observation most likely attributed to the immunomodulatory and antiviral effects of estrogen [43]. Under ART, women of reproductive age demonstrate comparable levels of cell-associated HIV-1 DNA to matched men, but significantly lower levels of cell-associated RNA (in isolated CD4+ T cells) and residual plasma HIV-1 RNA [44]. In Ugandan cohorts, the inducible replication-competent reservoir was smaller in women compared to men, suggesting sex-specific differences in reservoir dynamics. Mechanistically, these effects have been linked to oestrogen and its receptor, which suppress HIV-1 transcription and attenuate the efficacy of latency reversal agents (LRAs) in vitro [45]. This raises important considerations for sex-specific cure strategies.

Age

The composition and dynamics of the HIV reservoir are significantly influenced by age. In neonates and infants, initiating antiretroviral therapy (ART) early results in exceptionally small reservoir sizes, often characterized by slower viral reactivation [46]. This protective effect diminishes sharply if ART is delayed beyond the first year of life, particularly after age five. In contrast, the impact of advanced age on the reservoir is less defined [47]. Ageing is associated with immunosenescence and clonal expansion of antigen-specific T cells, which may lead to a reservoir that is increasingly clonal, concentrated in differentiated cell subsets and decays more slowly [48]. Together, these findings underscore that reservoir establishment and persistence follow distinct biological pathways at opposite ends of the lifespan [49].

HIV subtype

The influence of viral subtype on reservoir persistence is an underexplored but critical dimension. Most reservoir research has centred on subtype B, which predominates in resource-rich regions but represents a minority of global infections [34]. Direct comparisons between subtype B and non-B reservoirs are complicated by confounding factors, including disparities in ART access, co-infection burden, and host genetics. One comparative study reported a three-fold smaller reservoir in Ugandan patients (predominantly infected with non-B subtypes) compared to individuals in Baltimore, MD, though multiple contextual variables may have contributed [50]. Another cohort study suggested that subtype B infection may support larger reservoirs, mechanistically linked to the higher activity of the HIV-1 Nef protein in down-regulating HLA class I and evading immune clearance [51].

Co-infections and inflammation

HIV infection induces a state of chronic immune activation and systemic inflammation that persists during ART [34]. Damage to the gut mucosa results in translocation of microbial products into circulation, fuelling inflammation [20]. Concurrently, HIV-driven immunodeficiency increases the burden of co-infections such as Cytomegalovirus (CMV), further sustaining immune activation [34]. Most studies suggest that heightened immune

activation correlates with larger reservoirs [29]. These observations collectively indicate that chronic inflammatory states, whether driven by HIV itself, co-infections, or microbial translocation, substantially modulate reservoir dynamics [20]. Consequently, regional variations in co-infection prevalence and inflammatory burden may critically shape reservoir size and composition, with important implications for the design and efficacy of cure strategies [34]. Intensive research in diverse epidemiological contexts is therefore urgently required.

1.3 Potential prospects in reservoir control and eradication strategies

Recent findings from animal models suggest that a functional cure for HIV may be achievable through a variety of approaches, either as standalone strategies or in combination [1]. Promising strategies include inducing potent antiviral CD8+ T cell responses, CCR5 receptor deletion, and the administration of bNAbs [1]. Studies on bNAbs have shown remarkable potential, however, the extensive genetic diversity of HIV poses a major challenge to the success of this strategy [1]. Thus, in-depth characterization of the HIV reservoir, particularly the Env variants targeted by bNAbs is essential to inform and optimize future cure strategies [1].

1.3.1 Antiretroviral therapy

ART suppresses viral replication but cannot cure HIV due to the extremely slow decay of the viral reservoir, which is seeded primarily just before treatment begins [34]. This pre-treatment reservoir is unstable, and early ART initiation creates a critical, dynamic window by reducing immune activation and stabilizing a smaller pool of latently infected cells [34]. Leveraging this window with curative interventions is a key strategy. While some individuals exhibit small reservoirs or rapid decay, suggesting a functional cure might rarely occur, achieving widespread eradication likely requires enhanced strategies [34]. Promising approaches include combining ART with immune-stimulating therapies, bNAbs, or gene-editing techniques like CCR5 deletion [34]. However, the extensive genetic diversity of HIV, particularly in the viral envelope, remains a major obstacle for strategies like bNAbs, underscoring the need for detailed reservoir characterization [1].

1.3.2 Latency reversal

A central strategy for an HIV cure is "shock and kill," which uses LRAs to reactivate the latent virus for immune-mediated clearance [34]. First-generation LRAs often induced viral RNA but not robust protein or virion production, failing to reduce the reservoir due to weak potency and ineffective immune clearance [34]. Second-generation LRAs, such as second mitochondrial-derived activator of caspases (SMAC) mimetics, show more consistent reversal in preclinical models, offering promise for the development of potent future strategies. [52]. Immune-stimulatory strategies, including Toll-like receptor (TLR) agonists like TLR-7, have shown mixed results, while some studies indicated latency reversal or potential remission when combined with immunotherapy, their primary mechanism may be immune modulation rather than direct reactivation [53]. Cytokine-based strategies, such as those involving IL-15, are also under investigation [54].

1.3.3 Latency silencing

An alternative to “shock and kill” is the “block and lock” strategy, which aims to permanently silence the latent HIV reservoir by reinforcing transcriptional repression, akin to how human endogenous retroviruses are regulated [34, 55]. This approach is supported by evidence that latent proviruses can accumulate silencing epigenetic marks like DNA methylation [34]. Experimental attempts to accelerate this process, such as with the Tat inhibitor didehydro-cortistatin A (dCA), have shown modest effects in reducing reactivation [56]. More recent screening has identified new candidates like mechanistic target of rapamycin (mTOR) pathway inhibitors, but the long-term feasibility of achieving universal, irreversible silencing is uncertain due to reservoir heterogeneity [57].

1.3.4 Gene editing

Advances in gene editing offer the potential to directly target and excise or disrupt integrated proviruses [34]. In practice, however, this approach faces substantial challenges: proviruses are both rare and genetically diverse within a single host, complicating the delivery and specificity of editing tools [34]. More feasible targets may be host dependency factors such as CCR5, where genetic disruption can render cells resistant to infection without requiring precise targeting of proviral sequences [34]. Notably, even partial editing

of susceptible cells could reduce viral amplification to levels that blunt systemic rebound, though safe and efficient in vivo delivery remains a major hurdle [34].

1.3.5 Clonal proliferation

Clonal expansion of infected memory CD4+ T cells is a major mechanism sustaining the HIV reservoir [58]. Homeostatic cytokines like IL-7 can drive this proliferation, while drastic interventions like stem-cell transplantation can reduce it, though they are not broadly feasible [34].

Targeting proliferation specifically in infected cells represents a more feasible strategy. Ideally, interventions would inhibit expansion of infected clones while permitting uninfected memory T cells to proliferate, gradually diluting the reservoir [34]. Alternatively, therapies that eliminate chronic antigenic drivers of proliferation, such as CMV or microbial products from the gut, may reduce reservoir persistence. The reservoir's durability is rooted in long-lived, self-renewing stem and central memory T cells, making these subsets critical targets for future eradication strategies [34].

1.3.6 Immunotherapy

A parallel avenue of investigation seeks to harness or enhance HIV-specific immunity to eliminate infected cells during ART or maintain control post-treatment [34].

Immunotherapies that directly target cells expressing the envelop protein for killing are ideal candidates [34]. Immune checkpoint blockade has also been tested, inspired by successes in oncology. While early case reports suggested reduced HIV persistence, two NIH-sponsored clinical trials were terminated prematurely due to unacceptable toxicity, underscoring the need for refined dosing strategies [33]. More broadly, immunotherapeutic interventions face the dual challenge of overcoming immune exhaustion and avoiding collateral immune activation [33]. Another major approach involves engineered HIV-specific chimeric antigen receptor T (CAR-T) cells, which directly target cells expressing the viral envelope protein and have advanced into clinical trials [34].

A particularly prominent class of immunotherapy involves bNAbs directed against the envelope glycoprotein (Env) which have demonstrated robust in vivo suppression of replication, likely through blocking viral entry and spread [59]. Additionally, bNAbs may mediate antibody-dependent cellular cytotoxicity by targeting envelope expressed on the surface of infected cells. While in vivo evidence for direct reservoir clearance is limited, indirect markers suggest some effect [33]. However, bNAbs share a key limitation with other envelope-targeting strategies like CAR-T cells, their efficacy is contingent upon sufficient expression of the envelope protein on the surface of infected cells [34]. Additionally, the extensive genetic diversity of HIV poses a formidable challenge to any therapy targeting a specific viral antigen [34]. A thorough understanding of the genetic diversity and expression patterns of the HIV envelope is therefore paramount in predicting and enhancing the efficacy of bNAbs, as the success of this strategy is contingent on effectively targeting the variable and evolving antigenic landscape of the virus.

1.3.7 Broadly neutralizing antibodies

bNAbs are a special class of antibodies capable of neutralizing a broad spectrum of genetically diverse HIV strains by targeting conserved, often conformational, epitopes on the Env trimer [59]. This "breadth" distinguishes them from strain-specific neutralizing antibodies and is critical for countering the extreme antigenic diversity of HIV, which is a major obstacle for both vaccines and therapeutics [60]. bNAbs exert their primary antiviral effect by binding directly to the functional Env spike, thereby blocking the essential steps of viral entry attachment to the host cell CD4 receptor or co-receptor binding and fusion, and thus preventing the infection of new cells [61].

Beyond direct virus neutralization, bNAbs can engage the immune system's effector functions to eliminate infected cells [61]. By binding to Env proteins expressed on the surface of virus-producing cells, bNAbs can facilitate antibody-dependent cellular cytotoxicity (ADCC), where NK cells recognize the antibody-bound cell and induce its killing [62]. Furthermore, emerging evidence suggests that bNAbs may exert a "vaccinal effect" by forming immune complexes with viral antigens, potentially enhancing the host's own humoral and cellular HIV-specific immune responses, which could contribute to sustained viral control [63]

In the absence of an effective vaccine, passive immunization with bNAbs has emerged as a promising prevention and treatment strategy [59]. In animal models, bNAbs have demonstrated robust protection against acquisition, and early-phase human trials confirm favourable safety and pharmacokinetic profiles [59]. Moreover, in infected individuals, passive administration of bNAbs has delayed viral rebound after treatment interruption and suppressed viremia in untreated individuals [59].

The Antibody Mediated Prevention (AMP) trials provided proof-of-concept for the protective potential of bNAbs in humans but also revealed substantial challenges, including viral diversity, resistance, and the limited durability of antibody protection [64]. Consequently, current efforts are focused on enhancing the breadth, potency, and persistence of bNAbs through engineered variants, combinations, and novel delivery platforms such as long-acting formulations [64]. While unlikely to provide a stand-alone cure, bNAbs remain a cornerstone of next-generation strategies aimed at HIV prevention and potential eradication [64].

1.4 HIV-1 Envelope

1.4.1 Structure of the HIV-1 Envelope and mechanisms of host cell entry

The target of broadly neutralizing antibodies is the HIV-1 Env spike, a trimeric complex on the virion surface responsible for orchestrating host cell entry [65]. This complex is composed of three gp120 surface subunits noncovalently associated with three gp41 transmembrane subunits, derived from the cleavage of a heavily glycosylated gp160 precursor [66]. The Env spike exhibits a sophisticated, layered architecture [67]. Structural analyses using cryo-electron microscopy and crystallography reveal a structurally invariant β-sandwich core at the gp120-gp41 interface, surrounded by three highly flexible layers and capped by a heavily glycosylated outer domain [68]. This design creates a balance between structural plasticity and functional constraint [68].

Viral entry is a multi-step process initiated by the high-affinity binding of gp120 to the host CD4 receptor, which triggers extensive conformational changes [69]. These

rearrangements expose the coreceptor binding site on gp120, allowing engagement with either CCR5 or CXCR4 [65]. This series of binding events destabilizes the gp120-gp41 association, releasing gp41 from its metastable, native conformation [65]. gp41 then transitions through a pre-hairpin intermediate state, where its fusion peptide inserts into the target cell membrane and its N-terminal regions form a coiled-coil scaffold [70]. The subsequent folding back of its C-terminal regions to associate with this scaffold creates a stable six-helix bundle, which pulls the viral and cellular membranes together to catalyse fusion and pore formation [71].

This entry mechanism presents defined therapeutic vulnerabilities, such as the targetable pre-hairpin intermediate inhibited by drugs like enfuvirtide (T-20) [72]. However, the dynamic and highly plastic nature of the Env spike is also fundamental to HIV-1's ability to evade neutralizing antibodies [73]. The heavy glycan shield and conformational masking of conserved epitopes allow the virus to maintain the essential gp120-gp41 interactions required for entry while continually adapting to escape immune pressure [74]. This structural and functional plasticity remains the central challenge for both therapeutic and vaccine design, directly informing the strategies needed to overcome immune evasion.

1.4.2 Immune evasion: escape from antibodies

HIV-1 Env is among the most variable proteins known in nature, largely due to extensive glycosylation [75]. Each trimer contains, on average, 93 potential N-linked glycosylation sites (PNGSs), which together account for approximately half of its mass and obscure nearly 70% of the protein surface from antibody recognition [76]. The number and positioning of PNGSs vary considerably both between and within individuals with dynamic shifts such as the commonly observed N332-to-N334 transition conferring resistance to V3-directed neutralizing antibodies [73]. In addition, glycan processing heterogeneity allows individual sites to be occupied by distinct glycoforms (different structural variants of glycans attached to the same glycosylation site), further complicating immune recognition [77].

This "glycan shield" represents a formidable barrier to humoral immunity, as host tolerance mechanisms often limit the development of effective anti-glycan antibodies [75].

Nonetheless, some individuals eventually develop bNAbs after prolonged infection and repeated rounds of viral escape [75]. These bNAbs converge on a limited set of conserved “sites of vulnerability” on Env, including the CD4-binding site, the V3 loop [78], the trimer apex, the gp120-gp41 interface, the fusion peptide, and the MPER. Importantly, bNAbs typically recognize epitopes comprising both protein and glycan elements, underscoring the complex interplay between structural conservation and variability [75].

However, even when potent bNAbs are elicited or administered, HIV-1 employs several strategies to escape their pressure. The most direct mechanism is epitope mutation, where amino acid substitutions or glycan shifts within the bNAb footprint abolish or severely reduce binding affinity [79]. Furthermore, the inherent conformational flexibility and dynamics of the Env trimer allow transient masking of conserved epitopes; bNAb epitopes may only be fully exposed during specific stages of the entry process, limiting the window for neutralization [80]. On a population level, the global diversity of HIV-1 means that a bNAb effective against one clade may be less potent against another due to natural sequence variation at key epitope residues, a phenomenon known as strain-specific resistance [81]. These escape mechanisms collectively ensure that viral subpopulations can persist and rebound under selective immune pressure, posing a significant challenge for both natural control and therapeutic bNAb applications [81].

The extraordinary variability of the Env region exemplifies the evolutionary race between HIV-1 and the host immune system [75]. While the identification of bNAb epitopes has provided valuable targets for vaccine design, the plasticity of the Env glycan shield, coupled with its capacity for rapid escape via mutation and conformational masking, continues to undermine efforts at developing universally effective interventions [75].

1.4.3 Sites of bNAb targeting on HIV-1 Envelope

Despite the formidable glycan shield and mutational escape that characterize HIV-1’s immune evasion, the virus must retain conserved, functional regions on its Env trimer to mediate cell entry [60]. These regions constitute the conserved "sites of vulnerability" targeted by bNAbs [60]. The identification and structural characterization of these sites

reveals how bNAbs overcome evasion by targeting epitopes where Env's mutational flexibility is constrained by function [79].

These vulnerable sites are defined by their location on the Env architecture and the specific bNAbs that engage them [82] (Figure 1.2). The CD4-binding site (CD4bs) is a conserved functional groove on gp120, bNAbs like VRC01 and N6 mimic the host CD4 receptor to block viral attachment, targeting a protein-centric epitope that includes a key glycan [83]. The V1V2-glycan site (trimer apex) is dominated by a dense glycan patch and bNAbs such as PG9 and CAP256-VRC26.25 use exceptionally long loops to penetrate this shield, binding a glycan-dependent quaternary epitope formed between adjacent gp120 protomers [84]. Other key sites include the gp120-gp41 interface, where bNAbs like PGT151 and 8ANC195 bind complex quaternary structures bridging both subunits [85], the fusion peptide, where antibodies like VRC34.01 target the exposed N-terminus of gp41 [86] and the MPER, a conserved stretch of gp41 bound by bNAbs like 10E8 that inhibit the final steps of membrane fusion [87].

Critically, most bNAb epitopes are not purely protein-based but are glycan-dependent, incorporating one or more host-derived glycans as essential components of the binding interface [60]. This strategy represents a unique adaptation, turning the virus's key defensive structure into a critical vulnerability [60]. However, the very constraints that make these sites vulnerable also dictate the modes of escape from bNAbs, such as glycan shift (N332 to N334) mutations at the V3 supersite or amino acid substitutions in the CD4bs [88]. Consequently, these sites are both the blueprint for vaccines and the frontline of viral escape, explaining why bNAb therapies typically require combinations [89].

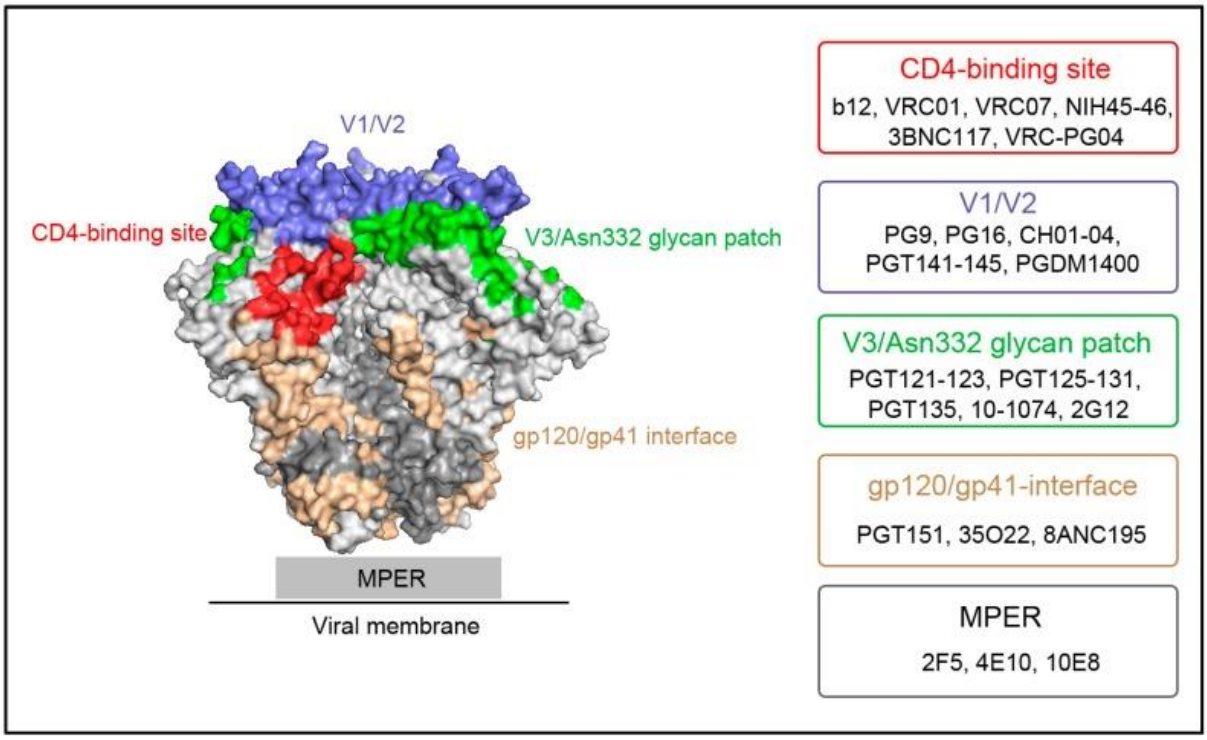

Figure 1.2 Classification of HIV-1 Neutralizing Antibodies. This figure summarizes the major bNAb classes and their epitope locations. The HIV-1 Env trimer is shown with its key domains: gp120 (surface subunit) and gp41 (transmembrane subunit). Several antigenic supersites targeted by bNAbs are indicated, along with representative antibodies for each region: the CD4-binding site (e.g., VRC01, VRC07), the V1/V2 glycan region (e.g., PG9, PGDM1400), the V3 and Asn332-glycan patch (e.g., PGT121, 10-1074), the gp120/gp41 interface (e.g., PGT151), and the MPER (e.g., 2F5, 10E8). This diagram was sourced from Zhang (2016) (Creative commons license: CC BY 4.0) [90].

1.5 Evidence for compartmentalization of Env

Since HIV-1 Env mediates cell entry and is the target of bNAbs, it will be important to assess whether there are genetic differences in Env between reservoir sites, and whether these viral genetic differences, if present, affect neutralization sensitivity by bNAbs.

Recent studies suggest that there may indeed be such genetic differences with the potential for differing neutralization sensitivity. HIV-1 compartmentalization has been reported across multiple tissue sites, including the CNS, GALT, and the male and female genital tracts [91]. The existence of genetically distinct viral populations in different anatomical niches poses significant implications for both vaccine design and cure strategies [91]. In a

study carried out by Wang et al. (2022), computational methods and Env sequence data from the blood and tissues of 7 terminally ill patients were used to map neutralization resistance patterns across 33 body compartments [92]. Results revealed that the mean neutralization sensitivities for each antibody were similar between compartments except for some antibodies that displayed altered sensitivity in the CNS [93]. There was also heterogeneity in neutralization sensitivities between antibodies, within individuals (several sequences were measured per individual) and between individuals [93]. There were, however, limitations to this study – since computational analysis was used, it did not confirm if the analysed *env* sequences were functional and it was also limited to a subtype B infected population.

In contrast to the study carried by [93], a key study investigating viral populations in paired blood and LN samples from individuals on long-term suppressive ART found little evidence for sustained genetic compartmentalization of the HIV-1 reservoir in LNs [94]. Using phylogenetic analysis of intact *env* sequences, the researchers showed that viral populations in the two compartments were largely intermingled, with most LN sequences closely related to viruses found in the blood [94]. They concluded that cellular proliferation of infected cells, rather than localized replication within a protected sanctuary, is the dominant mechanism maintaining the reservoir in LNs during ART [94]. This finding suggests that while lymphoid tissue is a major anatomical site of persistence, it does not necessarily function as an isolated, independently evolving compartment [94]. Neutralization assays were not however performed in this study to investigate whether there were neutralization sensitivity differences by compartment, and the study mainly focused on subtype B infection. Further investigation of the neutralization sensitivity of HIV-1 reservoir variants in non-subtype B regions of the world and their effect on bNAb sensitivity is therefore warranted, especially since HIV-1 subtype C is the most predominant subtype world-wide, and virus and host characteristics may differ between populations infected with different subtypes [95].

1.6 Study rationale

As detailed in the preceding sections, the development of a curative or remission-based strategy for HIV-1 faces a central, unresolved challenge: the persistence of a genetically diverse and stable viral reservoir that evades antiretroviral therapy and immune clearance.

While lymphoid tissues are established as critical anatomical sanctuaries for these reservoirs, the extent to which they harbour genetically compartmentalized and functionally distinct viral populations, particularly those with differing susceptibility to immune effectors remains unclear and debated.

bNAbs represent a leading immunotherapy with the potential to target this reservoir, as outlined in Section 1.3 and 1.4. However, their efficacy is intrinsically challenged by the extraordinary genetic and structural diversity of Env, its capacity for immune evasion Section 1.4.2, and the heterogeneous nature of the reservoir itself Sections 1.2.1 & 1.2.2. For bNAb-based strategies to succeed, they must neutralise not only actively replicating viruses but also the variants persisting in latent reservoirs, which may evolve under distinct selective pressures.

Notably, as reviewed in Section 1.5, preliminary evidence suggests that Env sequences can differ between anatomical compartments, with in silico predictions indicating these differences may alter neutralization sensitivity. However, in these studies, sensitivity was not directly measured, and one key investigation was conducted in individuals not on ART, thus not directly assessing the treatment-suppressed reservoir. Furthermore, the predominant focus of such research has been on populations infected with HIV-1 subtype B. As established in Section 1.2.4, reservoir dynamics and host-virus interactions are influenced by population-specific determinants, including viral subtype. Given that the most heavily burdened global populations are infected with non-B subtypes, primarily subtype C, there is a pressing need to characterise reservoir variants in this context to ensure the relevance and equity of future cure strategies.

Therefore, this study aims to address key gaps in our understanding of the HIV-1 reservoir in individuals infected with subtype C. Specifically, it investigates whether Env variants persisting in the reservoir, represented by LN and PBMC samples obtained at least one year after ART initiation, exhibit sequence differences compared with pre-therapy PL variants, and whether such differences may affect neutralization sensitivity to bNAbs. Env sequences from PL, PBMCs, and LN samples were characterised, with unique reservoir-specific mutations confirmed using next-generation sequencing. For a subset of participants, replication-competent viruses encoding patient-derived Env were generated, and their sensitivity to a panel of clinically relevant bNAbs was assessed in TZM-bl cells.

By linking genetic variation in the reservoir to functional neutralization profiles in this subset, this work contributes data that may be used to inform the design of effective, globally applicable bNAb therapies.

1.7 Study aims

- To investigate whether there are sequence differences, particularly those previously reported to alter neutralization sensitivity, between reservoir Env variants from PBMCs and LNs and pre-therapy plasma Env variants.
- To investigate whether there are differences in neutralization sensitivity between reservoir Env variants from PBMCs and LNs and pre-therapy plasma Env variants.

1.8 Study objectives

- Identify potentially unique reservoir variants by comparing already available patient-derived bulk Env sequences from pre-therapy plasma as well as from LNs and PBMCs obtained after 1 year of therapy (n=11 patients).
- Perform deep sequencing of the pre-therapy plasma samples to confirm whether the mutations identified in the reservoir were unique or whether they were already present at a low level in the pre-therapy plasma.
- For a subset of participants, generate replication-competent recombinant viruses encoding participant-derived Env from pre-therapy plasma and post-therapy PBMC and LN compartments.
- Investigate the antibody neutralization sensitivity of these viruses using TZM-bl cells and a panel of 9 clinically-relevant bNAbs.

Chapter 2 – Methods and Materials

2.1 Ethical approval

Ethical clearance for this study was obtained from the Biomedical Research Ethics Committee (BREC) of the University of KwaZulu-Natal (BREC/00007155/2024). Written informed consent was obtained from all participants prior to enrolment. LN samples were voluntarily excised following the approved LN study protocol (BF298/14).

2.2 Study participants

The study cohort comprised eleven HIV-1–infected individuals receiving ART, enrolled from two established Durban-based studies; namely, the Females Rising through Education, Support and Health (FRESH) cohort (BF131/11) and the HPP Acute Infection Cohort (BE102/14) [96] [95]. Briefly, these are observational, acute HIV infection cohorts in Umlazi, South Africa. Among the participants included in this study, five initiated ART during early infection, whereas the remaining individuals commenced therapy during the chronic stage of infection. Samples analysed in this study included pre-therapy plasma (PL) and post therapy LN and PBMCs that were closely matched in collection time (median of 553 days [453-765,5 days, IQR] for LN collection after ART initiation)(Table 2.1). The LNs were voluntarily excised in accordance with the approved LN study protocol (BF298/14). Pre-treatment PL samples were compared with LN and PBMC specimens obtained following ART initiation to assess genetic and neutralization sensitivity differences across compartments and treatment stages.

Table 2.1: Samples analysed from LNs, PBMCs and PL.

Participant ID	Treatment initiation	Treatment date	Plasma date	Lymph node date	PBMC date
594	Early	8/05/15	8/05/15	21/09/16	13/12/16
651	Early	9/08/15	9/08/15	30/11/16	29/09/16
683	Early	29/07/15	11/08/15	29/09/16	5/12/16
714	Early	21/09/15	28/09/15	29/10/16	10/11/16
1210	Early	9/05/17	9/05/17	6/09/17	16/10/17
093	Late	5/03/14	6/01/14	02/02/17	23/03/17
1012	Late	26/08/16	26/08/16	25/09/18	14/09/18
0039	Late	10/03/15	05/03/15	12/04/17	3/04/17

0037	Late	22/09/15	28/10/15	29/03/17	23/03/17
0098	Late	2/09/16	26/08/16	27/03/18	27/03/18
as33-3380	Late	22/10/12	30/08/12	21/06/18	03/04/18

2.3 Env single genome and bulk amplification

Amplicons (*env*) and bulk Sanger sequences had been previously generated from participant-derived samples. This historical sequencing data was used for assessing the genetic differences in the participant-derived viruses from PL, LN and PBMCs. Briefly, PL specimens stored at –80°C were thawed, and viral RNA was extracted from 140 µl of PL using the QIAamp Viral RNA Mini Kit (Qiagen, Hilden, Germany). For PL samples with viral loads below 10,000 copies/ml, centrifugation of 500 µl of PL was performed at 14,000 rpm for two hours prior to RNA extraction to enhance concentration of viral nucleic acids.

LN and PBMC samples, preserved in liquid nitrogen, were thawed before nucleic acid extraction. DNA was isolated from approximately 1 to 2 x 10^6 LN cells using the MasterPure Complete DNA and RNA Extraction Kit (Lucigen, Middleton, WI, USA), with cell pellets resuspended in 300 µL Tissue and Cell Lysis Solution according to the manufacturer's instructions. DNA extraction from 5 × 10^6 PBMCs was performed using the DNeasy Blood and Tissue Kit (Qiagen), with cells resuspended in 200 µL PBS prior to lysis. All extracted DNA samples were quantified using a nanodrop and stored at -20°C. Although the LN/PBMCs were collected approximately 8-10 years prior to this study and samples stored in liquid nitrogen, the nucleic acid extractions and initial PCR amplifications were done only 1-2 years after storage and the amplicons were stored at -20 °C. A description of the amplification steps carried out previously follows next. We thereafter performed the PCR reactions using 100 bp env primers in preparation for recombinant virus generation using the existing amplicons, as described in Section 2.5.1.

Following extraction, the viral RNA from PL was converted to complementary DNA (cDNA) to serve as a template for PCR amplification using the env-specific reverse primer OFM19 (5′-GCA CTC AAG GCA AGC TTT ATT GAG GCT TA-3′) for targeted cDNA synthesis. The reactions were assembled using two separate master mixes. Master Mix 1 consisted of 1 µL OFM19 primer (2 µM), 1 µL dNTP Mix (10 mM), and 2 µL of nuclease-free water per reaction. Master Mix 2 was composed of 4 µL 5x First Strand buffer, 1 µL 0.1M DTT, 1 µL RNaseOUT

(40 U/µL), and 1 µL SuperScript IV (200 U/ µL) per reaction. For the procedure, 4 µL of Master Mix 1 was aliquoted into individual 0.2 mL PCR tubes kept on ice, and 9 µL (concentration not determined) of extracted viral RNA was added to each tube. The first thermal cycling step was initiated with the following conditions: 65°C for 5 minutes, then 4°C for 1 minute. At the first programmed pause (Pause 1), the cycler was halted, and 7 µL of Master Mix 2 was added to each tube, bringing the final volume to 20 µL. The cycling then resumed with 55°C for 10 minutes, 80°C for 10 minutes, and 4°C for 1 minute. At the second pause (Pause 2), the cycler was halted again, and 1 µL of RNase H (on ice) was added to each tube, adjusting the final volume to 21 µL, before resuming the cycle for a final incubation at 37°C for 20 minutes followed by an indefinite hold at 4°C.

The full-length *env* gene was subsequently amplified from the cDNA (and DNA from tissue templates) using a nested PCR approach. The first round of PCR was performed using Platinum™ Taq DNA Polymerase High Fidelity (Invitrogen). The reaction mixture was assembled as follows: 2 µL 10X Buffer, 0.8 µL $MgSO_4$ (50 mM), 0.4 µL dNTP Mix (10 mM), 0.2 µL OFM19 primer (10 µM), 0.2 µL VIF1 primer (10 µM; 5′- GGG TTT ATT ACA GGG ACA GCA GA -3′), 0.1 µL Platinum HF DNA polymerase (5 U/µL), 15.3 µL nuclease-free water, and 2 µL cDNA template (concentration not determined). The thermocycling conditions for the first round consisted of an initial denaturation at 94°C for 4 minutes, followed by 35 cycles of 94°C for 15 seconds, 55°C for 30 seconds, and 68°C for 2 minutes, with a final extension at 68°C for 20 minutes.

For the second round of PCR, the Phusion High-Fidelity PCR system (New England BioLabs) was used. The reaction was assembled containing 5 µL 5X Phusion Buffer, 0.5 µL dNTP Mix (10 mM), 0.5 µL Env1A primer (10 µM; 5′- CAC CGG CTT AGG CAT CTC CTA TGG CAG GAA GAA-3′), 0.5 µL Env1M primer (10 µM; 5′- TAG CCC TTC CAG TCC CCC CTT TTC TTT TA -3′), 0.25 µL Phusion HF DNA Polymerase (2 U/µL), 15.8 µL nuclease-free water, and 2.5 µL of the first-round PCR product (concentration not determined) as template. The second-round PCR was performed with an initial denaturation at 98°C for 30 seconds, followed by 35 cycles of 98°C for 10 seconds, 65°C for 30 seconds, and 72°C for 2 minutes, and a final extension at 72°C for 10 minutes before a 4°C hold. The resultant PCR product was verified by agarose gel electrophoresis (1% agarose, 120V, 40 minutes), and the concentration of each sample was quantified using the nanodrop. This *env* PCR protocol was previously described in [97].

2.4 Genetic analysis of Env sequences

To address the first aim of the project, Env sequence differences between compartments were identified and assessed to determine whether any were previously reported to alter neutralization sensitivity.

2.4.1 Sanger sequencing

The *env* PCR products were previously bulk sequenced using the BigDye ready terminator kit v3.1 (Applied Biosystems) in combination with ABI 3130xl genetic analyser (Applied Biosystems) and thereafter edited using Sequencher v5 (Gene Codes, Ann Arbor, MI).

The previously generated Sanger sequences were utilized in this study to compare Env sequences derived from PBMC reservoirs, LN reservoirs, and pre-therapy PL. Sequence alignments were performed using GeneCutter (www.hiv.lanl.gov). Sequences were visualised in BioEdit to identify amino acids that differed between the compartments. Insertions with respect to the HXB2 strain were stripped out in BioEdit Sequence Alignment Editor, for correct codon numbering purposes. Maximum-likelihood phylogenetic trees were constructed using PhyML (www.hiv.lanl.gov) to assess the relatedness of the sequences to one another and to reference strains. The subtype C consensus sequence (2021) was obtained from the Los Alamos HIV sequence database.

2.4.2 Deep sequencing

Deep sequencing was conducted on all pre-therapy PL *env* amplicons to determine whether mutations identified within the reservoir, but not in pre-therapy PL by Sanger sequencing, were unique or already present in PL at low frequencies prior to therapy initiation. Briefly, plasma *env* amplicons were submitted to the KRISP sequencing facility, where deep sequencing was performed on an Illumina MiSeq platform using the appropriate Illumina library preparation kits. Only variants detected at a frequency of 2% and above were considered. These variants were detected using Geneious Prime. To evaluate the potential functional relevance of mutations unique to the reservoir, a list of mutations previously associated with altered neutralization sensitivity (Table 2.2) was consulted to assess whether any mutations unique to the reservoir occur at sites that may affect neutralization sensitivity.

Table 2.2: HIV-1 Env mutations previously associated with altered neutralization sensitivity.

Binding region	Amino acid position	Cons C AA[a]	Sensitivity	Resistance	References
V1V2	130-132 Glycan	NCT	130D/ Glycan removal	NxS/T	[98]
	156-158 Glycan	NCS	NxS/T	156K/ Glycan removal	[99]; [100]
	160-162 Glycan	NIT	NxS/T	160K, D/ Glycan removal	[99]; [101]; [102]
	161	I	I, M, A	V	[101]
	162	T	T, S		[103]; [104]
	164	E	D, E	G, S	[99]; [102]
	165	L	L, W, Y	A, I	[102]; [103, 104]; [105]
	166	R	R	G, S, T, Q, I	[102]; [105]
	167	D	D	T, G, N	[99]; [101]; [104]
	168	K	K	A	[99]
	169	K	K	E, V	[101]
	170	Q	Q	K	[101]; [102]
	171	K	K	E, R	[101]; [102]
CD4 Binding site	99	D	K	D	[102] ; [106]
	197	N	N, K	T	[107]; [101];[108]; [109]
	198	T		T	[109]; [106]
	199	S	S		[110]; [109]
	234-236 Glycan	NGT	Glycan removal[b]	NxS/T	[102]; [111]
	275	E	K	E, V	[112]; [102]; [106]
	276	N	N	A, D	[110]; [102]; [111]
	278	T	T	I, A	[79]; [113]; [111]
	279	N	N, D	K, D, A	[113]; [110];
	280	N	N	Y, D, S	[111]
	281	A	A, G, D	T	[113]; [112]
	282	K	K	A	[107]; [114]; [115]
	364	S	S, P	H	[102]
	365	S	S	K, A	[116]; [107]
	371	I	I	A	[102]; [107]
	372	T	V	A	[107]; [114]
	425	N	N	R, A	[102]; [115]
	429	E	K, R	G, E	[117]; [106]
	456	R	R	S, W	[102]; [111]
	458	G	G, Y	D	[102]; [118]; [113]

	459	G	G	D	[118]; [102]
	471	G	G	E, R	[102]; [113]
	474	D	D	A, N	[102]
	476	R	R	A	[116]
V3 Loop	137	A	S, O	D, V	[102]
	156	N	NxS/T	Glycan removal	[102]
	295-297 Glycan	VCT	NxS/T	295E, T, A / Glycan removal	[102]
	297	T	T		[102]
	300	N	N	Y, S, D, G	[102]
	301-303 Glycan	NNN	NxS/T	Glycan removal	[102]
	304	R	R		[102]
	307	I	I	A, V	[102]; [119]
	323	I	I	T, V	[102]
	324	G	G		[102]
	325	D	D	E, S, K, N	[102]; [109]
	328	Q	Q	K	[102]
	330	H	H	A, Y	[102]; [109]
	332-334 Glycan	NIS	NxS/T	Glycan removal	[102]
	386-388 Glycan	NTS	NxS/T	Glycan removal	[102]
	392-394 Glycan	NST	NxS/T	Glycan removal	[102]
MPER Region	671	N	N	T, S	[102]; [109]
	672	W	W	A, L	[102]
	673	F	F	L	[102]; [109]
	676	T	T	S	[102]
	674	D	D	A, S	[102]
	680	W	W	G	[102]
	683	K	K	R	[102]
gp120/gp41	276-278 Glycan	NLT	NxS/T	276D / Glycan removal	[102]; [113]
	279	N	D	N	[102, 120]; [121]
	501	A	A	L	[79]
	503	R	R	S	[83]
	611-613 Glycan	NSS	NxS/T	611 A, D / Glycan removal	[110]
	613	S	S	A	[79]; [110]
	637-639 Glycan	NYT	NxS/T	637A, K / Glycan removal	[79]; [110];
	639	T	T		[110]
	647	E	E	A, G	[110]; [122]
	648	D	E	K, R	[122]

[a] Consensus C amino acid.

[b] Mixed effect depending on antibody.

2.5 Neutralization sensitivity analysis of Env sequences

To address the second aim of the project, for a subset of the participants (n=6), viruses encoding the Env sequences were generated and analysed for neutralization sensitivity.

2.5.1 Generation of HIV-1 Env recombinant viruses

Recombinant viruses encoding patient-derived *env* sequences were generated by homologous recombination between a PCR-amplified *env* product and a linearized, *env*-deleted NL4-3 backbone in HEK293T cells (Figure 2.1).

Firstly, another round of PCR was performed on the existing *env* products (section 2.3) using primers designed for homologous recombination with the *env*-deleted NL4-3 backbone. These primers were designed to be complementary to the NL4-3 sequence immediately flanking the deleted *env* gene. The reaction master mix for each sample comprised of the following: 37 µL nuclease-free water, 2 µL (25 ng/µl) template DNA, 5 µL 10x High-Fidelity PCR Buffer, 4 µL of dNTPs (10 mM), 0.8 µL of each primer (10 µM) and 0.25 µL (5 U/µl) Taq HS polymerase. All components were stored at –20°C. PCR was performed using the following thermocycling conditions [1 cycle (94°C, 2 minutes), 40 cycles (94°C, 30 seconds, 60°C, 30 seconds, 72°C, 2 minutes), 1 cycle (72°C, 7 minutes)] with a final volume of 50 µL in each sample and the resultant PCR product was verified by agarose gel electrophoresis (1% agarose, 120V, 30 minutes) and purified using the QIAquick PCR Purification Kit (Qiagen) according to the manufacturer's instructions. The concentration of the purified DNA was quantified using a nanodrop.

The NL4-3 Δenv plasmid was linearized to allow for homologous recombination with the PCR-amplified *env* insert upon co-transfection into HEK293T cells. The plasmid was digested with BstEII, which cuts at a single site within the polylinker region where the *env* gene was deleted. The digestion reaction was assembled as follows: 17 µg NL4-3 Δenv plasmid, 5 µL 10x Restriction Enzyme Buffer, 0.5 µL 100X BSA, 3.4 µL BstEII enzyme (2 U/µg plasmid), and nuclease-free water to a final volume of 50 µL. The reaction was incubated at 60°C for 2 hours to ensure complete digestion. The linearized plasmid was verified by agarose gel electrophoresis (1%).

HEK293T cells were maintained under optimal conditions to ensure high viability and transfection efficiency. The cells were cultured in 13 mL of pre-warmed complete Dulbecco's Modified Eagle Medium (DMEM), supplemented with 10% fetal bovine serum (FBS), 5 mL L-glutamine (200 mM), 5 mL HEPES (1M) and 2.5 mL Penicillin-Streptomycin (10,000 U/mL). Cells were kept in a T75 flask in a humidified incubator at 37°C with 5% CO_2 and were passaged every 2-3 days upon reaching 80-90% confluence to maintain them in an exponential growth phase.

For each passage, the culture medium was aspirated and the cells were washed with 5 mL of pre-warmed PBS. The cells were then briefly treated with 1.5 mL of pre-warmed trypsin and incubated at room temperature for 2 minutes to facilitate detachment. After incubation, the detached cells were resuspended in 10 mL of complete DMEM. To quantify viable cells, a 10 µL aliquot of the cell suspension was mixed with 10 µL of trypan blue and analyzed using an automated hemocytometer (TC20, Bio-rad Laboratories Inc, Hercules, California). All procedures were performed in a bio-safety hood to maintain sterility.

For transfection, 0.5 x 10^6 cells/mL were seeded into each well of a 6-well plate in 2 mL of complete DMEM without antibiotics 18-24 hours prior to transfection, to achieve approximately 50-80% confluence at the time of transfection. After 24 hours, homologous recombination was initiated by diluting 1ug of the linearized NL4-3 backbone and 0.5 ug of the patient-derived *env* PCR product in 250 uL plain DMEM without additives and mixing gently in a 2 mL Eppendorf tube. In a separate tube, 8 uL (1 mg/mL)) of polyethylenimine (PEI) was mixed with 242 uL of plain DMEM without additives and incubated at room temperature for 5 minutes. The DNA-DMEM mixture was then added to the PEI-DMEM mixture and gently mixed 2-3 times followed by incubation for 20 minutes at room temperature to allow for DNA-PEI complex formation. Thereafter, 500 uL DNA-PEI complexes were added dropwise to the pre-seeded HEK293T cells in 6-well plates. The plate was gently swirled to ensure even distribution and returned to the 37°C, 5% CO_2 incubator. At 6 hours post-transfection, the media containing the complexes was aspirated and replaced with 1.5 mL of fresh complete media. The transfected cells were incubated for 48 hours to allow for recombination, viral assembly, and release. At 48 hours post-media change, the culture supernatant was carefully collected. The supernatant was clarified by centrifugation at 3000 rpm for 5 minutes at 4°C to remove cellular debris and the clarified supernatant, containing the recombinant virus stock, was aliquoted into cryovials and stored at -80°C.

To increase viral titres, the HEK293T-derived virus was used to infect CEM-derived GXR25 green fluorescent protein (GFP)-reporter T cells which express GFP upon successful HIV infection, allowing for the monitoring of infection via flow cytometry. GXR cells were cultured in T75 flasks containing 20 mL of R10 media, RPMI 1640 basal media supplemented with 10% FBS and 5mL Penicillin-Streptomycin (10,000 U/mL) and maintained at 37°C in a humidified 5% CO_2 incubator. Cell viability was monitored every 2-3 days by performing a cell count using the TC20, as described above. Once the cells reached a density of approximately 1 x 10^6 cells/ml, cells were pelleted by centrifugation at 3 000 rpm for 5 minutes. The supernatant was decanted, and the cell pellet was resuspended in pre-warmed R10 media at a concentration of 10 million cells/ml. For infection, 100 µL of the resuspended GXR cells were combined with 400 µL of thawed HEK293T-derived virus stock in a 24-well plate. The cell-virus mixture was then incubated for 24 hours at 37°C with 5% CO_2. After 24 hours, each well was supplemented with 1 mL R10 media and returned to the 37°C, 5% CO_2 incubator. There after infection was monitored every 48 hours by sampling a small aliquot of cells.

Briefly for each analysis, the cell suspension was mixed thoroughly using a serological pipette to ensure an even distribution, a 500 µL aliquot was then transferred into a cluster tube and replaced with 500 µL pre-warmed R10. The cluster tubes were then centrifuged at 1,500 rpm for 10 minutes followed by aspiration of the supernatants and resuspension of cell pellets in 4% paraformaldehyde (PFA). The samples were placed in a cluster tube box and covered with foil and kept at -4°C for 10 minutes, following which GFP expression was monitored by flow cytometry to determine the percentage of infected cells. Once 15–20% of the GXR25 cell population was GFP-positive, the cultures from the 24-well plate were transferred to T25 flasks containing 2 × 10^6 cells of fresh, uninfected cells in a final volume of 7 mL R10 media and the flasks were kept in the 37°C, 5% CO_2 incubator. After 24 hours, the volume in each flask was adjusted to 10 mL with additional media. The cells were monitored by flow cytometry every 48 hours, and virus stocks were harvested when 30% of the GXR25 T cell population was GFP-positive.

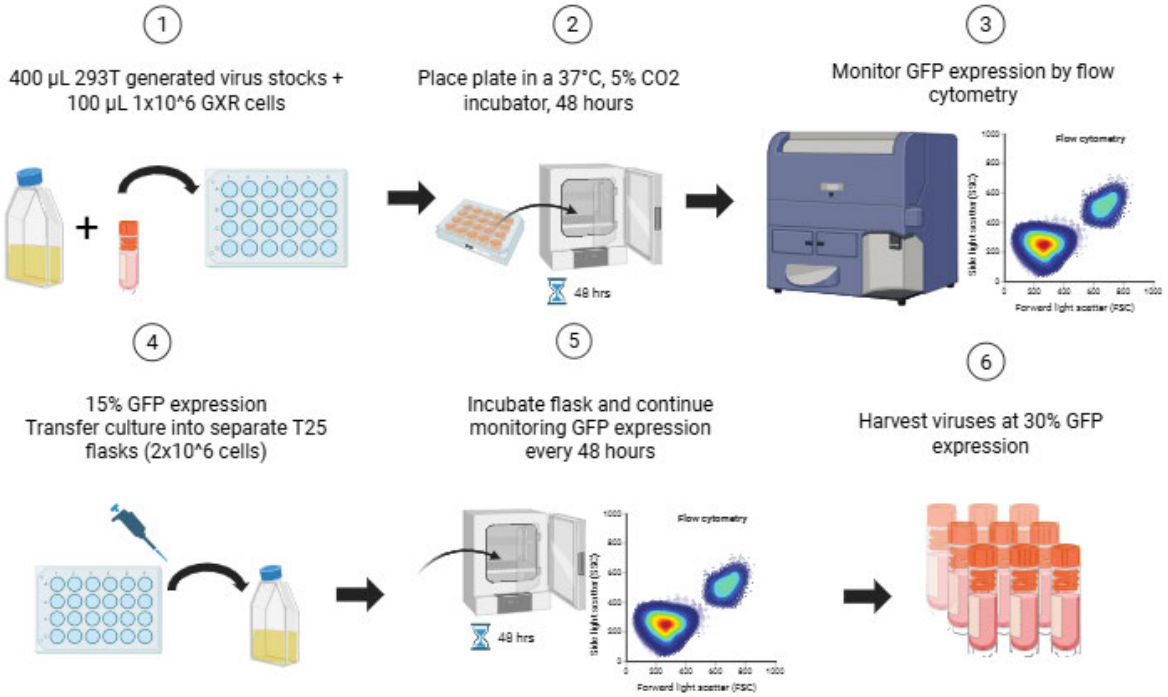

Figure 2.1. Viruses generated in HEK293T cells and their subsequent amplification in GXR cells. The schematic outlines the sequential process for amplifying viral titre using CEM-derived GXR25 T cells, which express GFP upon HIV-1 infection. **1.** In a 24-well plate, 100 µL of the concentrated GXR25 cells (1 million) are combined with 400 µL of thawed, HEK293T-derived recombinant virus stock **2.** The plate is incubated for 24 hours at 37°C with 5% CO_2. After the 24-hour incubation, 1 mL of fresh R10 media is added to each well **3.** Every 48 hours thereafter, an aliquot of the cell suspension is removed for analysis. The aliquot is centrifuged and, the pellet is fixed with 4% PFA, and GFP expression is quantified by flow cytometry **4.** Once flow cytometry detects 15–20% GFP expression, the entire contents of each well of the 24-well plate are transferred to separate T25 flasks containing 2 x 10^6 cells uninfected GXR25 cells in 7 ml R10. **5.** After 24 hours in the T25 flask, the culture volume is adjusted to 10 mL with additional R10 media. Infection is monitored every 48 hours by flow cytometry **6.** The amplified virus stock is harvested from the culture supernatant when approximately 30% of the GXR25 T cell population is GFP-positive.

2.6 Virus stock titration in TZM-bl cells

Each recombinant virus stock was titrated using a single-cycle infection assay in TZM-bl reporter cells to determine the infectious titre (Tissue Culture Infectious Dose [TCID] 50% per mL, TCID50/mL) prior to their use in neutralization assays, using methods similar to those previously described [96]. TZM-bl cells are engineered to express high levels of CD4, CCR5, and CXCR4, and contain an HIV-1 LTR-driven firefly luciferase reporter gene, allowing for sensitive quantification of infection via luminescence. The following protocol details the procedure.

On the day prior to infection, TZM-bl cells were harvested, counted using a TC20, and diluted to a concentration of 1 x 10^6 cells/ml in complete DMEM. A volume of 100 µL of this cell suspension, containing 10 x 10^4 cells, was seeded into each well of a flat-bottom, clear 96-well tissue culture plate to ensure the formation of a confluent monolayer (~70-90%) at the time of infection. The plate was incubated overnight at 37°C with 5% CO_2 to allow the cells to adhere. A 3-fold serial of dilution of each virus stock was prepared to capture a wide range of infectivity. The dilutions were prepared in plainDMEM, mixed well by vortexing and 70 µL of the virus dilutions were added in duplicates to the wells. All wells were topped up 30 µL with complete DMEM for a total volume of 200 µL in each well of the 96-well plate and then incubated for 48 hours at 37°C with 5% CO_2. A wild type NL4-3 strain was used as a positive control in each assay.

Infection was quantified 48 hours post-infection by measuring luciferase activity, which is directly proportional to the level of HIV-1 Tat-driven gene expression. After the 48-hour incubation, the plate was removed from the incubator, and 100 µL culture medium was aspirated from all wells. Following aspiration, 100 µL of Bright-Glo™ Luciferase Assay Reagent (Promega, Madison, WI, USA) was added to each well. The plate was then incubated at room temperature for 2 minutes to ensure complete cell lysis and a stable luminescent signal. A volume of 150 µL of the lysate from each well was transferred to a corresponding well of a black 96-well assay plate to optimize luminescence detection, and chemiluminescence was measured immediately using a PerkinElmer Victor Nivo luminometer.

2.7 Neutralization assay

Neutralization activity was assessed by measuring the reduction in virus infection of TZM-bl cells following a single round of infection, using Tat-regulated firefly luciferase (Luc) reporter gene expression as previously described [123] (Figure 2.2). The sensitivity of participant-derived Env variants to a panel of nine bNAbs targeting distinct epitopes, CD4 binding site (VRC01, VRC07-523LS, N6), V2 apex (CAP256-VRC26.25, PGDM1400), V3-glycan supersite (PGT121, 10-1074), MPER (10E8), and gp120-gp41 interface (PGT151) was evaluated.

To do this, each bNAb was reconstituted to a working stock solution of 200 µg/mL. On the day of the assay, 25 µL of complete DMEM was pipetted into all wells of a 96-well plate except (H3-H12), while 33.8 µL of complete DMEM was added into wells H3-H12. Thereafter, 7.5 µL of each bNAb was added in duplicate wells of row H (wells H3-H12). A 3-fold serial dilution of each bNAb was prepared in the 96-well plate by transferring 12.5 µL serially from row H (H3-H12) to row A (A3-A12). The starting concentration for each bNAb was 20 µg/mL and the lowest concentration was 0.009 µg/mL.

Each participant-derived recombinant virus stock was thawed and diluted in assay medium to a target concentration of 20,000-60,000 Relative Luminescence Units (RLU). 25 µL of each of the diluted virus stocks was then added to all wells of the plate, except the negative control wells in column 1, and then the plate incubated for 1 hour at 37°C with 5% CO_2 to allow for the virus-antibody binding to occur prior to cell infection. For the virus control (VC) wells, in column 2, 25 µL of plain DMEM was combined with 25 µL diluted virus. Following the virus-antibody incubation, 20 µL of cells (1 x 10^6 TZM-bl cells were prepared in 2 mL DMEM supplemented with (28 µL DEAE-Dextran) were added to the plate. TZM-bl cells without virus served as negative controls (column 1), while virus only wells (column 2) served as positive controls. The plate was then incubated for 24 hours at 37°C with 5% CO_2. After 24 hours, 130 µL of complete DMEM was added into all wells and the plate was incubated for a further 24 hours at 37°C with 5% CO_2. Following this, luciferase activity was measured as described above (section 2.6). The average RLU for the VC and cell control (CC) wells were calculated. The percent neutralization for each bNAb dilution was calculated using the formula: % neutralization = [1 - (RLU Test Well - RLU CC) / (RLU VC - RLU CC)] * 100, where the "Test Well" is the RLU from a well containing both virus and bNAb. The % neutralization

values were plotted against the log10 of the bNAb concentration. A non-linear regression curve (sigmoidal dose-response model) was fitted to the data using Microsoft Excel. The inhibitory concentration that resulted in 50% neutralization was calculated from the fitted curve for each virus and bNAb combination.

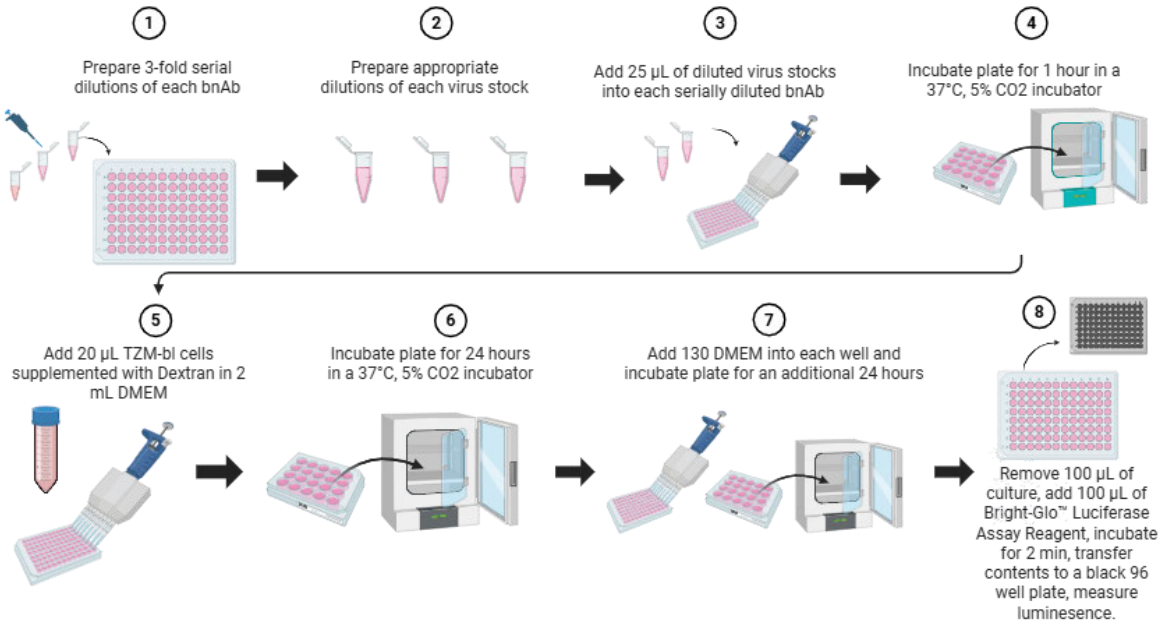

Figure 2.2. TZM-bl based micro-neutralization assay. The figure outlines the sequential steps for evaluating the neutralization activity of bNAbs against recombinant HIV-1 viruses using a single-round infection assay with TZM-bl reporter cells. The assay tests a panel of nine bNAbs targeting distinct Env epitopes, the CD4 binding site (VRC01, VRC07-523LS, N6), V2 apex (CAP256-VRC26.25, PGDM1400), V3-glycan supersite (PGT121, 10-1074), MPER (10E8), and the gp120-gp41 interface (PGT151). **1.** Each bNAb is serially diluted 3-fold across a 96-well plate in complete DMEM **2.** Each participant-derived recombinant virus stock is thawed and diluted in assay medium to a target infectivity of 20,000–60,000 Relative Luminescence Units (RLU) **3.** A 25 µL aliquot of each diluted virus stock is added to the wells containing the serially diluted bNAbs (except cell control wells) **4.** The plate is incubated for 1 hour at 37°C in a 5% CO_2 incubator to allow antibody-virus interaction **5.** Following incubation, 20 µL of TZM-bl cells (prepared at 1 x 10^6 cells in 2 mL of DMEM supplemented with DEAE-Dextran) are added to each well. Column 1 contains cells only (negative control), and column 2 contains virus and cells without antibody (virus control/positive control) **6.** The plate is incubated for 24 hours at 37°C with 5% CO_2 to allow viral entry **7.** After 24 hours, 130

µL of pre-warmed complete DMEM is added to each well, and the plate is returned to the incubator for an additional 24 hours **8.** After a total of 48 hours, 100 µL of culture medium is removed from each well and replaced with 100 µL of Bright-Glo™ Luciferase Assay Reagent and the contents are transferred to a black 96-well plate, and luminescence is measured.

2.8 Statistical analysis for neutralization data

Neutralization IC50s were compared across compartments (pre-therapy PL, PBMC reservoir, and LN reservoir) for each antibody. Pairwise comparisons between two compartments at a time were performed using the Wilcoxon signed rank test.

Chapter 3 – Results

3. Results

The reservoir is composed of latently infected cells that harbour replication-competent virus, which can reinitiate infection upon therapy interruption. A critical question is whether the viral populations residing in these reservoirs are similar to the pre-therapy virus or if they have evolved under selective pressures, potentially harbouring variants with altered sensitivity to immune responses, including bNAbs that target the HIV-1 Env protein. To address this, we characterized the HIV-1 Env sequences from pre-therapy PL and post-therapy reservoirs from 11 study participants. The analysis aimed to confirm the phylogenetic relationship between participant viruses from different compartments, quantify the genetic differences in reservoir viruses from the pre-therapy founder, identify mutations that were unique to the reservoir and whether these were associated with changes in bNAb sensitivity and finally, to functionally assess their neutralization sensitivity to a panel of bNAbs that target the CD4bs, V2 Apex, V3 glycan, MPER region, and the gp120-gp41 interface.

3.1 Phylogenetic analysis

We first sought to confirm the origin of the viruses persisting in the reservoir and to ensure that the bulk PCR amplified sequences derived from different participants were distinct. To achieve this, a phylogenetic analysis was performed to assess the relatedness of full-length *env* sequences obtained from PL, PBMCs, and LNs of the enrolled participants.

A maximum-likelihood phylogenetic tree was constructed from 30 bulk *env* sequences. The sequences were color-coded by participant to visualize their clustering. As shown in Figure 3.1, sequences from all three compartments (PL, PBMC, and LN) form distinct, participant-specific clusters. This clear clustering confirms that the viruses isolated from the PBMC and LN reservoirs originate from the same participant as the corresponding PL virus and are not the result of cross-participant contamination or sample mix-up. This confirms that any subsequent genetic or phenotypic differences observed between compartments are specific to each participant's viral population and can be attributed to viral evolution and/or compartmentalization. In addition, it was observed that two sequences from the reservoir (0039 PBMC and 1012 LN) were hypermutated, where hypermutation was confirmed using the

Hypermut tool from the LANL database, and these were therefore excluded from downstream genetic and functional comparisons.

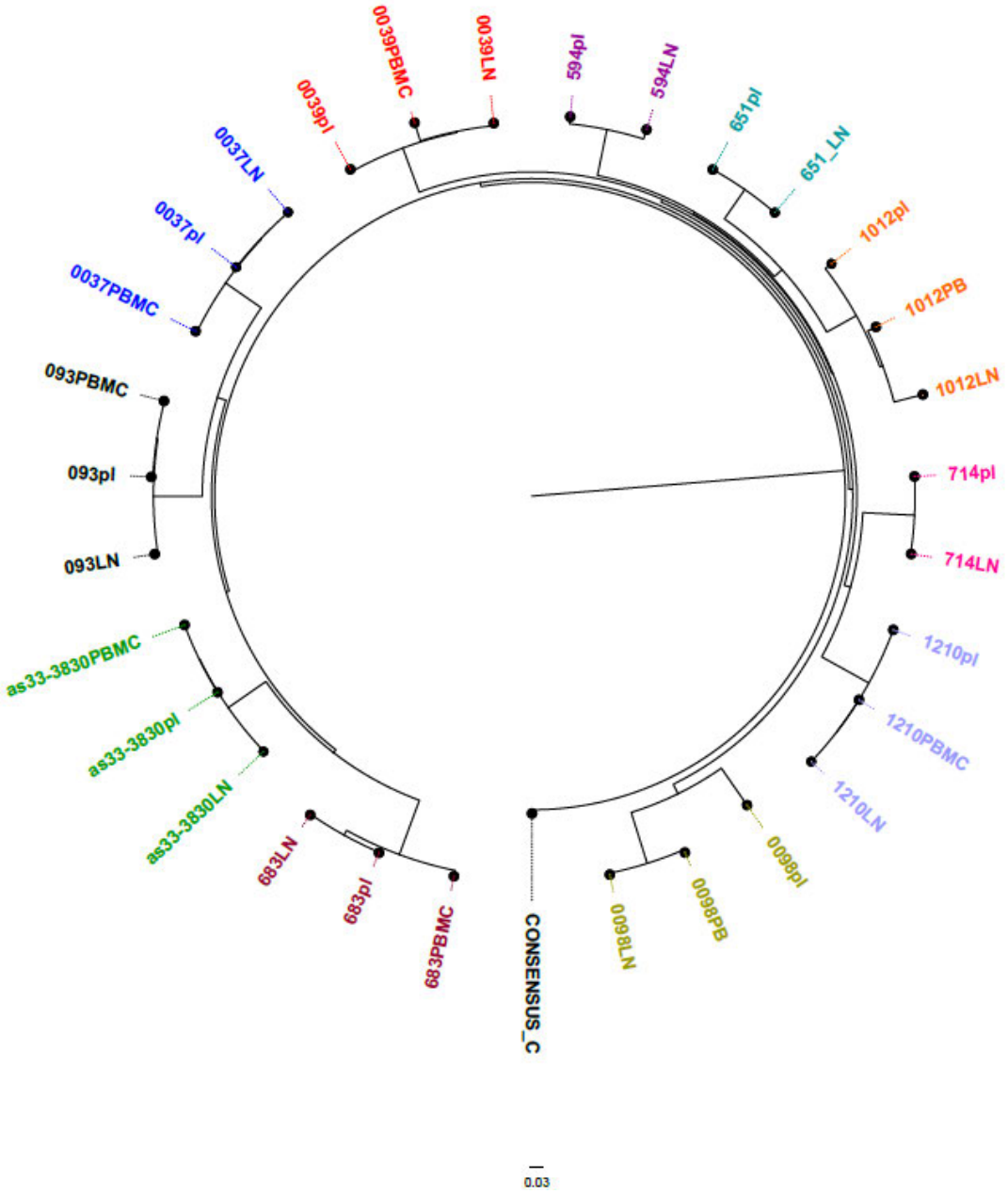

Figure 3.1. Phylogenetic relatedness of HIV-1 *env* sequences from pre-therapy plasma and post-therapy reservoirs. A maximum-likelihood phylogenetic tree was constructed using PhyML from 30 full-length *env* bulk nucleotide sequences derived from 11 study participants. The pre-therapy PL, PBMC, and LN sequences are color-coded by participant to illustrate their origin. The tree demonstrates that for each participant, sequences from all compartments form distinct clusters (indicated by participant-specific colors and labels), confirming that the viruses from the PBMC and LN reservoirs originate from that same participant as the pre-therapy PL

virus population. The HIV-1 subtype C consensus sequence from 2021 (Consensus_C) was obtained from the Los Alamos National Laboratory HIV Sequence Database as a reference.

3.2 Sanger and deep sequencing analyses

Having confirmed that reservoir sequences cluster with the pre-therapy plasma viruses from the same participant, we next investigated their genetic divergence from the pre-therapy PL virus. The analysis, summarized in Figure 3.2A, quantified the amino acid changes that emerged in the reservoir by comparing bulk Sanger sequences from the LN and PBMC compartments to the pre-therapy PL sequence. The median number of amino acid differences between the LN/PBMC reservoir and plasma sequences was 6 (IQR: 3-22.5) and 19 (IQR: 7-49) respectively. We additionally wished to quantify the number of these amino acid changes that occurred at residues previously reported to alter sensitivity to bNAbs (Table 2.2) to investigate whether or not there is any evidence for differences in neutralization sensitivity between compartments. A median of 0 (LN) and 2 (PBMC) of these mutations occurred at positions previously reported to alter sensitivity to bNAbs.

Of interest was whether mutations identified within the reservoir were already present as low frequencies in the pre-therapy viral population, or whether they were unique to the reservoir, either as a result of pre-therapy compartmentalization or emergence during therapy. To address this, deep sequencing was conducted on all PL *env* amplicons. As shown in Figure 3.2B, we observed a measurable number of unique mutations in the reservoir sequences (black). Specifically, 63% (LN; median = 3 and IQR = 1.25-15.25) and 73% (PBMC; median = 14 and IQR = 6-35) of mutations in the reservoir sequences were confirmed to be unique to the reservoir by deep sequencing. As observed previously, a very small minority of these reservoir specific mutations were found to occur at amino acid positions previously reported to alter sensitivity to bNAbs (blue).

Taken together, these results indicate a wide range in the amount of amino acid differences between pre-therapy Env variants and reservoir Env variants, with a substantial proportion of these being unique to the reservoir. However, very few of these differences are at residues previously reported to alter bNAb sensitivity.

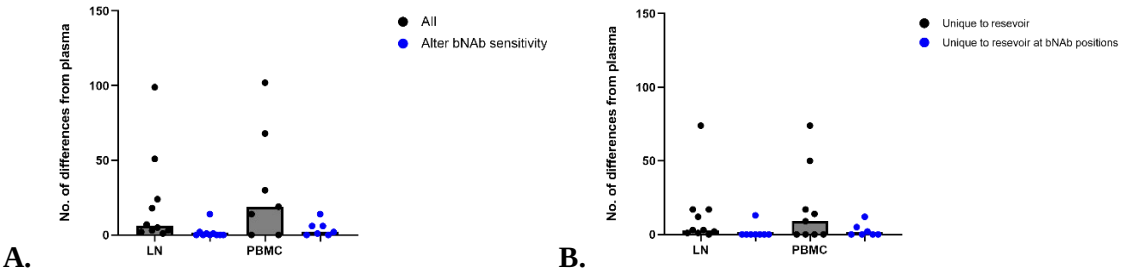

Figure 3.2. Genetic differences between reservoir-derived and pre-therapy plasma Env sequences. A. The graph quantifies the average number of amino acid differences between the pre-therapy plasma Env sequence and the sequences derived from the LN and PBMC reservoirs after at least one year of ART (black). A subset of these differences was further analysed to identify those occurring at known bNAb positions (blue), representing amino acid positions previously reported to alter sensitivity to bNAbs. **B.** The graph quantifies the total number of unique amino acid mutations in the reservoir sequences (black), as determined by deep sequencing of the pre-therapy plasma virus, and the subset of these unique mutations occurring at known bNAb sites (blue). Bars indicate the medians.

3.3 Differences in neutralization sensitivities between PL, LN and PBMC viruses

The observed genetic divergence between the Env variants from pre-therapy plasma and the reservoir, especially at bNAb sites, prompted further analysis to directly assess the functional neutralization sensitivity of viruses from different compartments. To do this, a subset of n=6 participants, representing a range of sequence divergence (low to high) between compartments, was selected. These participants were also chosen based on the successful generation of replication-competent viruses encoding env sequences from pre-therapy PL, PBMCs, and LNs. . These viruses were tested against a panel of nine bNAbs targeting five major epitope regions using a micro-neutralization TZM-bl based assay. The assay was repeated twice for each participant-derived virus and, an average of the two IC50s was recorded.

The resulting IC50 values are presented as a heatmap in Figure 3.3. The data shows a complex pattern of neutralization sensitivity, with distinct profiles observed across compartments and participants. Notably, no uniform pattern of increased or decreased sensitivity was observed in one compartment over another. Instead, the sensitivity was highly variable and dependent on the specific participant, the compartment from which the virus was derived, and the bNAb tested. For instance, some PBMC-derived viruses showed increased resistance to certain

bNAbs compared to their matched PL virus (e.g. the sensitivity of the 093 PL and PBMC virus to PGT151), while for other bNAbs, PBMC-derived viruses were more sensitive or similar in bNAb sensitivity to their PL virus counterparts (e.g. sensitivity of 093 PL and PBMC viruses to CAP256 and PGT121, respectively). Similar observations were made when comparing the LN and PL viruses. This heterogeneity is visually apparent from the pattern of red (sensitive), orange (less sensitive) and white (resistant) shading across the heatmap. To further visualise the compartment-specific differences in neutralization, a direct, antibody-by-antibody comparison of IC50 values for viruses from the PL, PBMC, and LN compartments was performed (Figure 3.4). The scatter plots in Figure 3.4 bNAb further highlight that there are no consistent and significant patterns of bNAb sensitivity differences between compartments (Wilcoxon signed rank test).

		CD4 binding site			V2 Apex		V3 Glycan		MPER	Interface
PID	Compartment	VRC01	VRCO7	N6	CAP256	PGDM1400	PGT121	10-1074	10 E 8	PGT151
3830	Plasma	0,11	0,12	0,06	0,01	0,15	0,40	20,00	4,96	0,66
	Lymph node	0,13	0,01	0,08	20,00	2,08	20,00	20,00	0,20	0,06
	PBMC	0,15	0,04	0,08	20,00	7,75	20,00	20,00	0,40	0,09
683	Plasma	0,03	0,06	0,15	20,00	0,84	20,00	20,00	0,04	0,12
	Lymph node	0,27	0,04	0,18	20,00	5,51	20,00	20,00	0,40	0,19
	PBMC	0,17	0,02	0,09	20,00	11,95	20,00	20,00	0,13	0,09
00-98	Plasma	0,03	0,01	0,13	20,00	5,72	20,00	20,00	0,01	0,07
	Lymph node	0,06	0,05	0,14	20,00	4,86	20,00	20,00	0,42	0,10
	PBMC	0,24	0,06	0,11	20,00	5,69	20,00	20,00	0,23	0,18
00-39	Plasma	0,25	0,04	0,13	20,00	8,75	20,00	20,00	0,34	0,19
	Lymph node	0,04	0,04	0,12	20,00	0,80	20,00	20,00	0,28	0,07
651	Plasma	0,56	0,13	0,29	0,02	0,60	2,60	2,17	18,15	0,15
	Lymph node	0,12	0,02	0,11	20,00	0,81	20,00	20,00	5,46	0,06
093	Plasma	3,41	0,06	0,66	20,00	16,28	0,01	0,05	17,09	0,04
	PBMC	7,86	0,47	1,49	0,09	3,15	0,02	0,05	20,00	20,00

IC50 titers	µg/ml
	<0,1
	0,1-0,9
	1,0-3,0
	3,1-9,9
	>10

Figure 3.3. Neutralization sensitivity of the 12 recombinant viruses to nine broadly neutralizing antibodies. A heatmap depicting the 50% inhibitory concentration (IC50) values for recombinant viruses encoding *env* sequences from PL, PBMCs, LN reservoirs tested against a panel of nine bNAbs. Antibodies are grouped by their target epitope: CD4bs (VRC01, VRC07-523LS, N6), V2 apex (CAP256-VRC26.25, PGDM1400), V3-glycan supersite (PGT121, 10-1074), MPER (10E8), and gp120-gp41 interface (PGT151). The colour scale represents the degree of sensitivity, with darker shades (red) indicating higher potency (lower IC50, greater sensitivity) and lighter shades (orange) indicating resistance (higher IC50, lower sensitivity). White cells represent conditions where neutralization was not detected (IC50 > 10 µg/ml).

CD4 Binding site

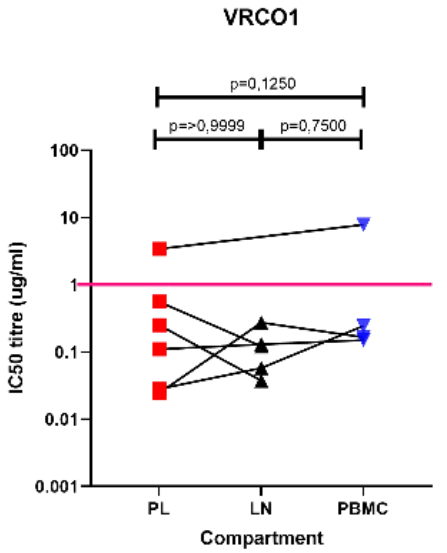

A.

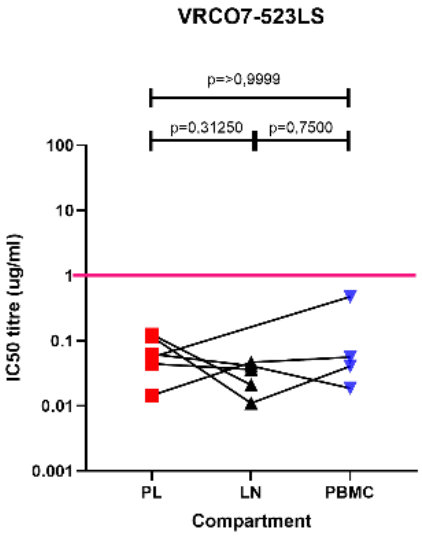

B.

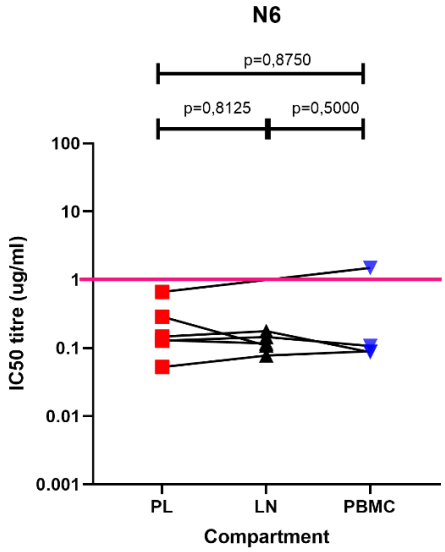

C.

V2 Apex

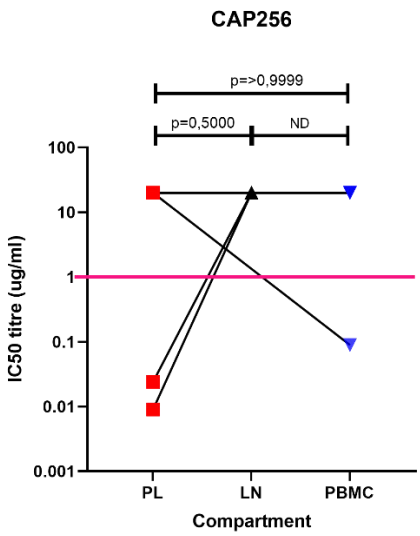

D.

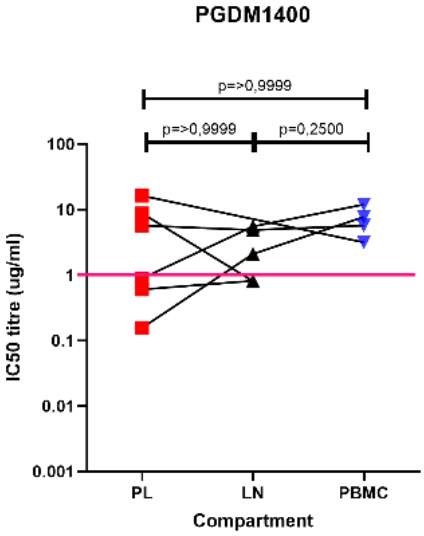

E.

V3-Glycan supersite

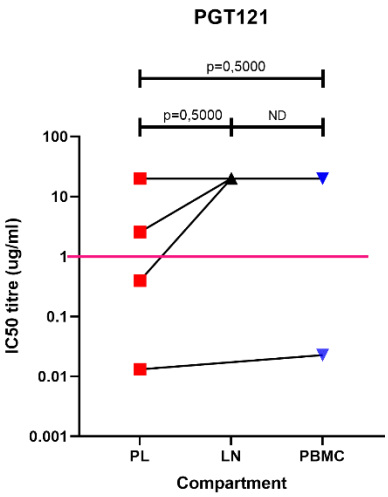

F.

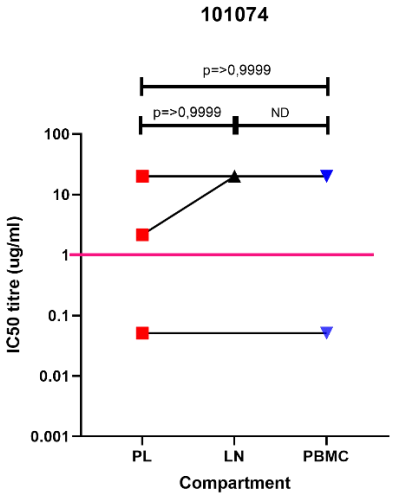

G.

MPER / gp120-gp41 interface

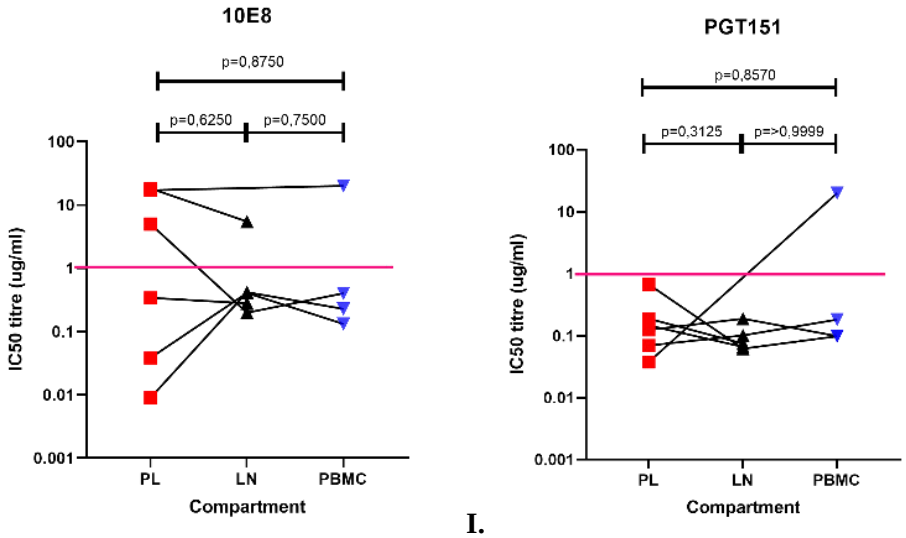

H. **I.**

Figure 3.4. Comparative neutralization sensitivity of viral variants across anatomical compartments. Paired dot plots comparing the IC50 values for recombinant viruses derived from PL (red), PBMCs (blue), and LN (black) reservoirs against a panel of bNAbs. Each point represents the IC50 value for a single participant's virus from the indicated compartment. The bNAbs target distinct epitopes, **(A-C)** CD4bs (VRC01, VRC07-523LS, N6), **(D-E)** V2 apex (CAP256-VRC26.25, PGDM1400), **(F-G)** V3-glycan supersite (PGT121, 10-1074), **(H)** MPER (10E8), and **(I)** gp120-gp41 interface (PGT151). *ND, not done as each row has the same difference.

3.3.1 Differences in neutralization sensitivities by antibody

It was notable that, overall, most viruses were sensitive to the CD4 binding site antibodies regardless of compartment, with IC50s ranging from 0.009-7.86 µg/ml (median = 0.11; IQR = 0.05 – 0.17; Figures 3.3 and 3.4). Similarly, all viruses, with the exception of one (20 µg/ml), were sensitive to the interface antibody (median = 0.1; IQR = 0.07 – 0.18). On the other hand, resistance to V2 and V3 antibodies was more common, and varied between compartments, with IC50s >10 ug/ml in 80% (CAP256), 13.3% (PGDM1400) 73.3% (PGT121), and 80% (10-1074) of the viruses. There were mixed results for the MPER antibody, where most of the viruses were sensitive to the MPER with the exception of two viruses.

3.4 Summary of HIV-1 Env epitope signatures affecting bNAb sensitivity

The phenotypic differences in neutralization observed in Figures 3.3 and 3.4 are likely driven by specific genetic changes in the *env* gene. We therefore noted the presence of known non-consensus mutations, at positions known to affect bnAb sensitivity, in the sequences that were included in the neutralization assays (Table 3.1). This table compiles Env amino acid positions from gp120 and gp41 that have been experimentally demonstrated to affect bNAb sensitivity across multiple epitope classes, including the V2-apex, V3-glycan supersite, CD4bs, the MPER region of gp41, and selected glycan-shield–associated positions.

Table 3.1 Summary non-consensus amino acids at HIV-1 Env positions known to affect sensitivity to bNAbs.

PID	V2 apex	V3	CD4bs	MPER	Interface
093PL	L161T, l165I, K169T, K171Q	A137T, V295N, 1307V, D325N, NST392GTH (glycan disrupted)	T198S, E429K, D474N	N671S, D674S	N279D, D648E
093PB	I161T, L165I, K171Q	A137T, V295N, I307V, D325N, NST392GTR (glycan disrupted)	T198S, E429K, D474N	N671S, D674S	N279D, D648E
683PL	Q170K	A137T, V295T, T297A, I307V	E429K	N671A	S613T
683LN	Q170K	A137T, V295T, T297A, I307V	E429K	N671A	S613T
683PB	Q170K	A137T, V295T, T297A, I307V	E429K	N671A	S613T
0039PL	I161T, K169R, Q170K, K171N	A137I, N300G, Q328K, NST392TNT (glycan disrupted)	D99S, T198S, I371V, E429G, D474N	D674S	N279D, K503R, D648E
0039LN	I161T, K169R, Q170K, K171N	A137I, N300G, Q328K, NST392TNT (glycan disrupted)	D99S, T198S, I371V, E429G, D474N	D674S	N279D, K503R, D648E
3830PL	E164V, Q170H	A137N, T297I, H330Y, NIS332TVN (glycan disrupted), NST392KGT (glycan disrupted)	A281V, I371V, E429R, D474N	D674N	
3830LN	E164V, Q170H	A137N, T297I, H330Y, NIS332TVN (glycan disrupted), NST392KGT (glycan disrupted)	A281V, I371V, E429R, D474N	D674N	

3830PB	E164V, Q170H	A137N, T297I, H330Y, NIS332TVN (glycan disrupted), NST392KGT (glycan disrupted)	A281V, I371V, E429R, D474N	D674N	
0098PL	K169R	A137N, T297V, N300G, I307T, Q328K, NIS332NIR (glycan disrupted), NST392NDN (glycan disrupted)	NGT234NGK (glycan disrupted), I371V, R456H, G458T, G459E, G471I	D674N	
0098LN	I161M	A137S, N300G, I307V, H330Y, NIS332TIN (glycan disrupted), NST392TEG (glycan disrupted)	T278A, A282I, S364H, I371V, G459S	N671S, D674S, K683R	D648K
0098PB	I161M, R166S	A137S, N300G, I307V, H330Y, NIS332TIN (glycan disrupted), NST392TEG (glycan disrupted)	NGT234DGT (glycan disrupted), T278A, S364H, G459S	N671S, D674S, K683R	D648K
651PL	I161A, E164A, L165I, Q170T	A137N, V295M, T297I, N300G, NIS332TIN (glycan disrupted)	A282IV, E429R, del456N, D474N, R476K	D674S, T676S	N279D, T639S, D648V
651LN	I161A, E164A, L165I, Q170T	A137N, V295M, T297I, N300G, NIS332TIN (glycan disrupted)	A282IV, E429R, del456N, D474N, R476K	D674S, T676S	N279D, T639S, D648V

Green indicates a mutation reported to be associated with sensitivity to the bNAb category.

Red indicates a mutation reported to be associated with resistance to the bNAb category.

Black indicates a mutation for which the effect on bNAb sensitivity is currently unknown or not well-characterized.

The neutralization data show distinct patterns of resistance and sensitivity across compartments and participants. The non-consensus mutations observed in the sequences (Table 3.1) partly explain some of the neutralization patterns, while other patterns are not clearly explained by the sequence data. The clearest link is between disruption of the N332 glycan motif and high-level resistance to the V3-glycan bNAbs 10-1074 and PGT121 (e.g., PIDs 3830 and 00-98). Indeed, several V3 antibody resistance mutations were present in the sequences, and most viruses were resistant to the V3 antibodies, although this was not the case for PID 093 despite the presence of resistance mutations. Another example where the mutations present are not in alignment with the neutralization sensitivity data is PID 0039, which was sensitive to the 10E8 antibody despite the presence of the known resistance mutation D674S (with no other non-

consensus mutations observed that have been previously reported to affect neutralization sensitivity to MPER antibodies). A genotype-phenotype misalignment was also observed with the loss of CAP256-VRC26.25 sensitivity in the V2 apex of 3830 and 651 LN and PMBC viruses post-ART despite no new mutations (at the known literature escape sites) having been identified (Table 3.1). Similar observations were made for the same samples concerning loss of sensitivity to the V3 glycan bNAbs and for 093 PBMC sensitivity to the PGT151 interface bNAb.

Chapter 4 – Discussion

4.1 Introduction

The persistence of replication-competent HIV-1 within cellular and anatomical reservoirs remains the principal barrier to an HIV cure [124]. Lymphoid tissues, particularly LNs, are established as major sites of reservoir persistence, providing structural, immunological, and pharmacological sanctuaries that facilitate long-term viral maintenance [29]. bNAbs represent a leading immunotherapeutic strategy to target and clear these reservoirs, but their efficacy is fundamentally challenged by the extensive genetic diversity of Env and the potential for compartmentalized evolution within reservoir sites [59]. While compartmentalization of viral populations has been reported in some studies, its functional impact on bNAb sensitivity especially in the context of globally prevalent non-B subtypes like subtype C remains inadequately characterized [91, 93].

This study aimed to address these gaps by (1) identifying sequence differences, particularly within known bNAb epitopes, between reservoir (PBMCs and LNs) and pre-therapy PL Env variants in individuals with HIV-1 subtype C infection, and (2) functionally assessing whether these genetic differences are associated with altered neutralization sensitivity against a panel of bNAbs.

Our key sequence findings confirm participant-specific clustering of viruses from all three compartments, indicating a common origin. While we identified a number of unique amino acid mutations in the reservoir compartments, very few of these occurred at positions previously associated with altered bNAb sensitivity. Functionally, we observed no consistent compartment-wide pattern of altered neutralization sensitivity between PL, PBMC, and LN-derived viruses across the six participants tested. Instead, neutralization profiles were highly variable and participant-specific. The following discussion interprets these findings, explores potential biological mechanisms, and considers the implications for bNAb-based cure strategies.

4.2 Genetic differences between pre-therapy plasma and reservoir Env sequences

Our phylogenetic analysis demonstrated that Env sequences from pre-therapy PL, PBMCs, and LNs formed distinct, participant-specific clusters. This confirms that the viruses that the viruses

from the different compartments all belong to the same individual and rules out cross-sample contamination or mix-ups.

We observed measurable genetic differences, with a median of 6 and 19 amino acid differences between pre-therapy PL and the LN and PBMC reservoirs, respectively. Deep sequencing revealed that a significant proportion (63% in LN, 73% in PBMC) of these mutations were unique to the reservoir and not detected as minor variants in the pre-therapy PL population. The origin of these unique mutations is a subject of ongoing debate. Two mechanisms are plausible, pre-ART compartmentalization or low-level ongoing replication during ART [34].

Pre-ART compartmentalization proposes that distinct viral populations are seeded in different tissues (e.g., lymphoid follicles, gut-associated lymphoid tissue) early in infection, driven by tissue-specific selective pressures such as localized immune responses or target cell availability [91]. Low-level ongoing replication, particularly in pharmacologically privileged sites like LNs where drug concentrations can be suboptimal, offers another explanation [41]. This continued evolution under selective pressure, potentially including residual immune pressure, could generate unique variants not present in the archived pre-therapy PL population. While some studies in macaques provide evidence against ongoing replication during ART [40], the question in humans, especially in tissue sanctuaries, remains open [34]. Our data cannot distinguish between these mechanisms, but they confirm that the reservoir harbours variants distinct from the pre-ART virus.

Notably, very few of the unique reservoir mutations occurred at amino acid positions known to affect bNAb sensitivity. This result is somewhat expected since the study participants were not given bNAbs and the result may also suggest that the reservoir is not strongly shaped by neutralizing antibody pressure. Instead, the unique reservoir mutations may be driven by other factors such as immune selection by CTLs, which can target infected cells even during latency, or by the fitness requirements for viral persistence in specific cellular environments (e.g., resting memory T cells) [19]. The small number of unique reservoir mutations that are known to affect bNAb sensitivity may suggest similarity between pre-therapy viruses and reservoir viruses in terms of bNAb sensitivity, however the presence or absence of known bNAb escape mutations does not necessarily predict phenotypic resistance. Thus, a subset of participants, who displayed a range of sequence differences between compartments, were selected for direct

comparison of neutralization sensitivity between compartments through virus generation followed by testing for sensitivity to a panel of clinically relevant bNAbs.

4.3 Neutralization sensitivity: compartment and antibody-specific patterns

4.3.1 Lack of consistent compartment wide differences

A central finding of our study is the absence of a uniform pattern of increased or decreased neutralization sensitivity in viruses derived from one anatomical compartment (PBMC or LN) compared to pre-therapy PL. Frequently, compartments had similar IC50s for a particular bNAb, while in other instances there was either an increase or decrease in the IC50 of reservoir viruses relative to the pre-therapy PL. Overall, in paired analyses, there were no statistically significant differences in neutralization sensitivity by compartment.

A computational study by Wang et al. (2022) [67], similarly reported comparable mean IC50s (considering each specific bNAb separately) across several different tissue compartments in untreated individuals, with the exception of the CNS compartment in some individuals where there was altered resistance for some of the antibodies. There are several differences between the current study and the study by Wang et al. (2022) worth noting. First, Wang et al. (2022) used in silico prediction based on Env sequence data from terminally ill, untreated patients, whereas our study measured actual phenotypic sensitivity using functional viruses from individuals on suppressive ART. The absence of ongoing replication and immune selection during ART may homogenize sensitivity profiles that were once compartmentalized. In addition, Wang et al. (2022) predicted the IC50s of multiple sequences per compartment and obtained a mean IC50 while our study measured the IC50 of a virus derived from a single bulk sequence per compartment. Second, our study focused on subtype C, while theirs was on subtype B, and fundamental virological differences between subtypes may influence compartmentalization dynamics [51]. Finally, by analysing only two reservoir compartments (PBMC and LN) we may not capture the full heterogeneity present across all body tissues.

4.3.2 High sensitivity to CD4-binding site (CD4bs) and interface bNAbs

The neutralization data revealed clear, antibody-class-specific patterns that are consistent with the known structural and functional constraints. Viruses from all compartments and participants were generally sensitive to CD4bs bNAbs (VRC01, VRC07-523LS, N6) and the gp120-gp41 interface bNAb PGT151. This is mechanistically expected. The CD4bs is one of the most functionally constrained regions of Env, as it must engage the host CD4 receptor with high affinity [69]. This constraint severely limits its mutational flexibility, making it a conserved and reliable target for bNAbs [125]. Similarly, the gp120-gp41 interface, targeted by PGT151, is involved in essential structural interactions for trimer integrity and fusion progression, imposing functional limitations on variation [83]. The conserved nature of these epitopes makes CD4bs and interface bNAbs attractive candidates for therapeutic combinations [125].

4.3.3 Variable and reduced sensitivity to V2 apex and V3-glycan bNAbs

In contrast, we observed widespread resistance or reduced sensitivity to bNAbs targeting the V2 apex (CAP256-VRC26.25, PGDM1400) and the V3-glycan supersite (PGT121, 10-1074). This variability is a feature of these epitope classes [99]. The V2 apex is a highly glycosylated, conformationally flexible region where immune pressure often drives sequence variation and glycan shifts [126]. For instance, the loss or shifting of key glycans at positions N156 or N160 is a well-documented escape pathway from V2 apex bNAbs [102]. This highlights the complex quaternary architecture of the apex, which can be disrupted by distant mutations or conformational masking [127].

The most consistent genotype-phenotype link in our study was for the V3-glycan supersite. High-level resistance to PGT121 and 10-1074 was associated with the disruption of the pivotal N332 glycan motif (e.g., in PIDs 3830 and 0098). The N332 glycan is a critical component of the epitope for these bNAbs [126]. Its loss is a major escape mechanism frequently observed in vivo [128]. However, resistance was not exclusively linked to N332 disruption, as some resistant viruses retained the N332 glycan but exhibited alterations at other glycan sites, including the N392–394 motif. On the other hand, PID 093 remained sensitive to V3-glycan bNAbs despite disruption of the N392–394 glycan motif and the presence of additional mutations previously associated with resistance. Together, these findings indicate that, within

this cohort, sensitivity to V3-glycan bNAbs cannot be attributed to a single glycan position but rather reflects the combined effects of multiple glycans and local Env structural features. While the sample size is limited, this observation is consistent with the known structural complexity of Env–antibody interactions. This underscores the complexity of glycan-dependent epitopes, in which the presence, processing, and spatial arrangement of multiple glycans collectively determine interactions with bNAbs [77]

Our observed neutralization profiles, particularly the high-level resistance to CAP256-VRC26.25 in 80% of viruses, appear more pronounced than the broad sensitivity and neutralization breadth reported for this antibody against subtype C viruses in recent literature, such as the longitudinal study in adults by Mandizvo et al. (2022) [96] and among infant transmitted/founder (TF) viruses (Ndlovu et al., 2025) [123]. An important methodological consideration is the virus platform used. Our study employed replication-competent recombinant viruses generated via homologous recombination in an NL4-3 backbone and amplified in T-cell lines. In contrast, many high-throughput neutralization datasets are generated using Env-pseudotyped viruses (PSVs) produced by co-transfecting Env and backbone plasmids in 293T cells [129]. Neutralization outcomes can differ between virus platforms due to differences in Env density, glycan processing, and spike conformation [89]. Replication-competent virions produced from T-cells may more closely reflect native Env organization compared to Env-pseudotyped viruses, which can have heterogenous Env incorporation [130]. Sensitivity to bNAbs targeting quaternary epitopes, such as the V2 apex, is particularly influenced by Env density and spatial arrangement on the virion surface [99] - its activity may be especially sensitive to these platform-dependent differences, potentially contributing to the higher levels of resistance observed here [131].

4.4 Implications for bNAb-based cure strategies

Based on our results, which identified antibodies targeting the CD4-binding site (e.g. VRC07) and interface (PGT151) as most potent against reservoir-derived variants. This finding is broadly consistent with prior observations. Ndlovu et al. (2025) also reported high overall sensitivity of both adult and infant transmitted/founder subtype C viruses to the CD4bs bNAbs VRC07. Mandizvo et al. (2022) similarly reported broad sensitivity to CD4bs VRC07 antibody as well as the gp120-gp41 interface PGT151 antibody. However, a notable distinction between

our study and both these studies is the considerable resistance we observed to V3-glycan targeting antibodies (PGT121 and 10-1074) and the V1V2 antibody CAP256-VRC26.25, which previously demonstrated notably higher neutralization breadth against subtype C viruses than was observed in this study.

Our findings carry significant implications for the design of bNAb therapies aimed at reservoir clearance and post-ART control. The broad sensitivity to CD4bs and interface bNAbs suggests that these classes should form a component of combination bNAb therapy for subtype C. Their conserved targets minimize the risk of pre-existing resistance in the reservoir. In contrast, the variable sensitivity to V2 apex and V3-glycan bNAbs suggests they should be used selectively, likely guided by pre-screening of an individual's reservoir sequences for key motifs (e.g., intact N332 glycan). With the exception of VRC07, no single bNAb in our panel neutralized < 1 µg/ml all viruses from all compartments in any participant. This reinforces the critical need for combinations of bNAbs targeting non-overlapping epitopes to prevent escape and achieve broad coverage, a principle well-established in the field [89].

The lack of consistent, compartment-specific neutralization sensitivity in the reservoir is encouraging. It suggests that the latent viral variants have not undergone compartment-specific bNAb escape [93], which may simplify the bNAb approach and increase the likelihood that administered bNAbs will be effective against rebound-competent viruses.

4.5 Study limitations and future directions

While this study provides valuable insights, certain limitations must be acknowledged. The sample size (n=11 for genetic comparisons, n=6 for phenotyping) is limited, though typical for intensive tissue-based reservoir studies. This limits the generalizability of our findings, and rare cases of strong compartmentalization may have been missed. Our functional analysis was performed on bulk-amplified *env* sequences, which represent the dominant variant from each compartment. This approach may mask the presence and phenotype of minor viral variants within the reservoir that could contribute to rebound. Future studies employing single-genome amplification paired with deep phenotypic screening would capture this heterogeneity. We examined only two reservoir compartments (PBMCs and a single LN). The reservoir is distributed across multiple tissues (CNS, gut, genital tract), and our findings may not represent

all sanctuary sites. The use of a laboratory derived backbone NL4-3 for generating recombinant viruses, while standard, may influence Env incorporation and function compared to a fully matched patient-derived backbone.

Future research could build on this work by, (1) expanding to larger, diverse cohorts to confirm the generalizability of these findings across subtypes and populations, (2) applying single-cell or near-full-length proviral sequencing techniques to correlate the genetic intactness and phenotype of individual reservoir proviruses, (3) investigating the role of antibody effector functions (e.g., ADCC) in clearing infected cells expressing these reservoir Env variants, as neutralization alone may not fully predict bNAb therapeutic activity [62], and (4) exploring *in vivo* models to test whether the neutralization profiles we observed in vitro correlate with the ability of bNAbs to prevent viral rebound or suppress reservoir-derived viremia.

4.6 Conclusion

In summary, this study provides genetic and functional characterization of HIV-1 subtype C Env variants from pre-therapy PL and post-therapy cellular reservoirs. We found that while reservoir sequences harbour some unique mutations, these differences rarely involve critical bNAb epitopes. Functionally, neutralization sensitivity is highly variable between individuals but does not follow a consistent pattern based on anatomical compartment (e.g. PBMC vs LN). While some clear genotype-phenotype links were observed for V3-glycan bNAbs, known resistance mutations did not necessarily predict phenotype, highlighting the importance of phenotypic assays to predict neutralization sensitivity. The neutralization sensitivity results underscored the suitability of the CD4bs and interface as promising therapeutic targets for bNAb therapy and reinforced the rationale for combination bNAb regimens. Overall, this work contributes to our understanding of the HIV-1 reservoir in subtype C infection and provides insights that may inform future bNAb-based strategies aimed at controlling or clearing the viral reservoir.

Appendix I – Plagiarism report

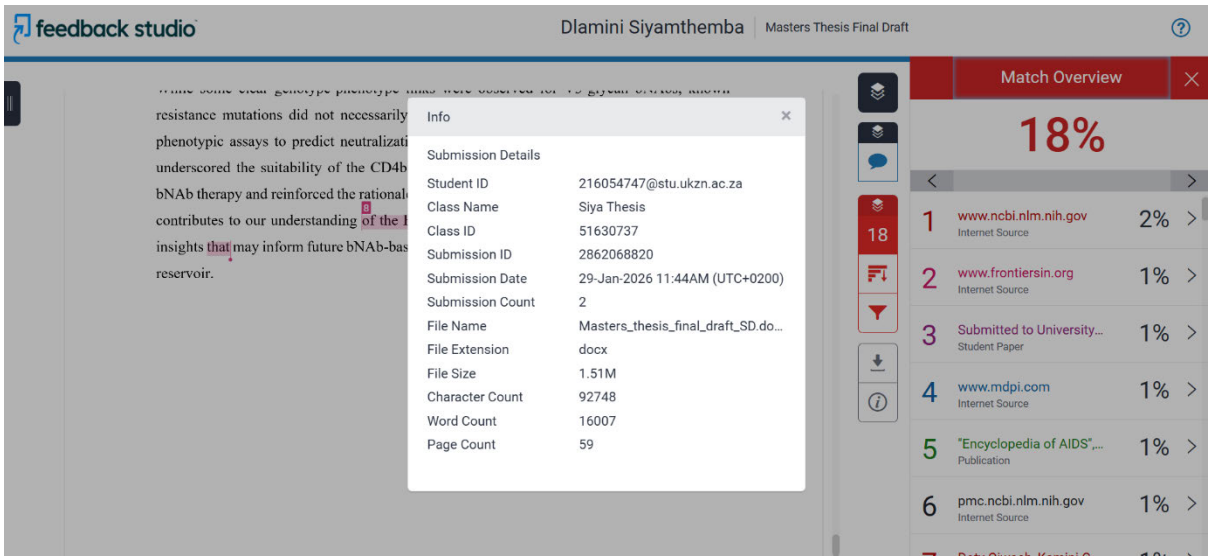

Appendix II – Current ethical approval letter for HPP Acute study

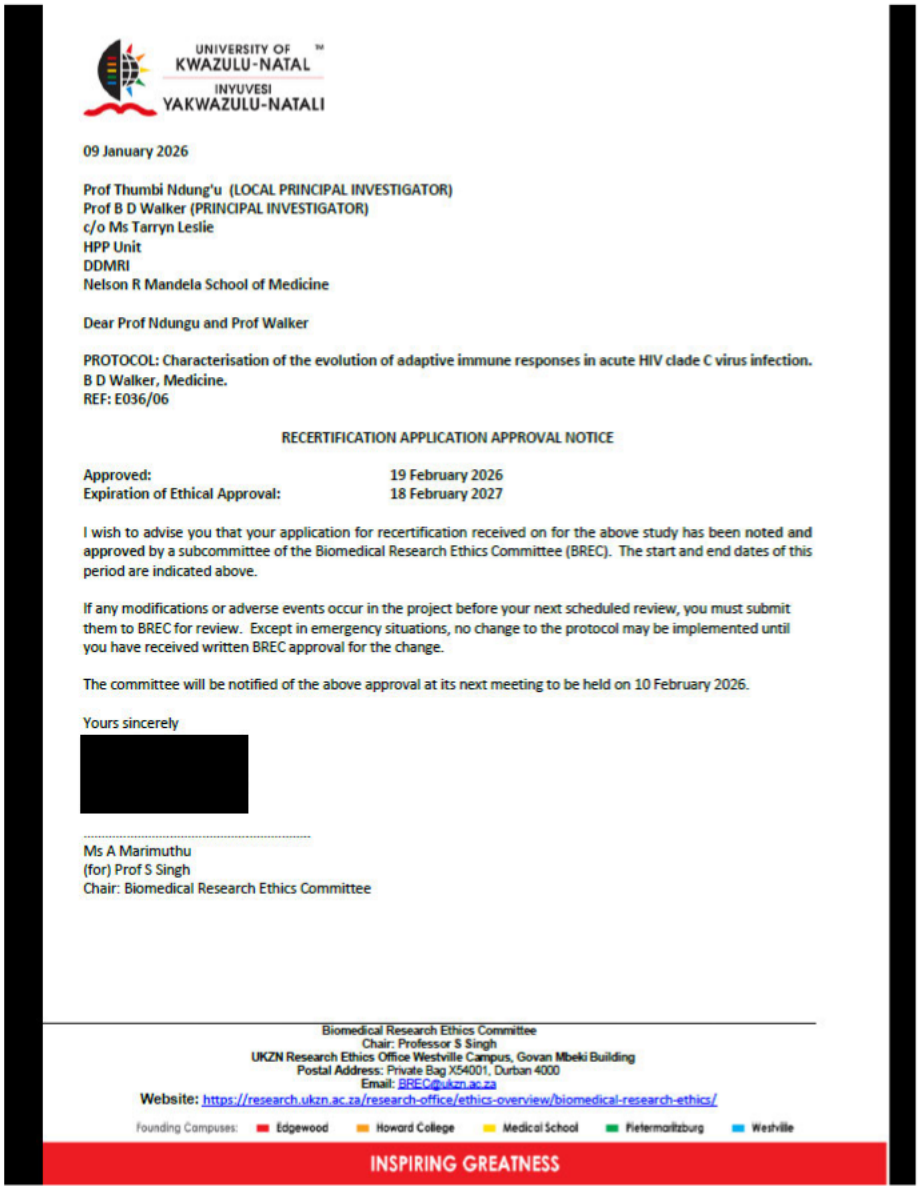

UNIVERSITY OF KWAZULU-NATAL
INYUVESI YAKWAZULU-NATALI

09 January 2026

Prof Thumbi Ndung'u (LOCAL PRINCIPAL INVESTIGATOR)
Prof B D Walker (PRINCIPAL INVESTIGATOR)
c/o Ms Tarryn Leslie
HPP Unit
DDMRI
Nelson R Mandela School of Medicine

Dear Prof Ndungu and Prof Walker

PROTOCOL: Characterisation of the evolution of adaptive immune responses in acute HIV clade C virus infection.
B D Walker, Medicine.
REF: E036/06

RECERTIFICATION APPLICATION APPROVAL NOTICE

Approved: 19 February 2026
Expiration of Ethical Approval: 18 February 2027

I wish to advise you that your application for recertification received on for the above study has been noted and approved by a subcommittee of the Biomedical Research Ethics Committee (BREC). The start and end dates of this period are indicated above.

If any modifications or adverse events occur in the project before your next scheduled review, you must submit them to BREC for review. Except in emergency situations, no change to the protocol may be implemented until you have received written BREC approval for the change.

The committee will be notified of the above approval at its next meeting to be held on 10 February 2026.

Yours sincerely

[redacted]

Ms A Marimuthu
(for) Prof S Singh
Chair: Biomedical Research Ethics Committee

Biomedical Research Ethics Committee
Chair: Professor S Singh
UKZN Research Ethics Office Westville Campus, Govan Mbeki Building
Postal Address: Private Bag X54001, Durban 4000
Email: BREC@ukzn.ac.za
Website: https://research.ukzn.ac.za/research-office/ethics-overview/biomedical-research-ethics/

Founding Campuses: Edgewood Howard College Medical School Pietermaritzburg Westville

INSPIRING GREATNESS

Appendix III – Current ethical approval letter for Lymph Node study

UNIVERSITY OF KWAZULU-NATAL
INYUVESI YAKWAZULU-NATALI

19 June 2025

Dr Zaza Ndhlovu
School of Laboratory Medicine and Medical Sciences
University of KwaZulu-Natal
ndhlovuz@ukzn.ac.za

PROTOCOL: Immune responses in lymphoid tissues of HIV positive individuals:
Non-Degree.
BREC REF: BF298/14.

RECERTIFICATION APPLICATION APPROVAL NOTICE

Approved: 14 July 2025
Expiration of Ethical Approval: 13 July 2026

I wish to advise you that your application for Recertification for the above protocol has been noted and approved by a sub-committee of the Biomedical Research Ethics Committee (BREC) for another approval period. The start and end dates of this period are indicated above.

If any modifications or adverse events occur in the project before your next scheduled review, you must submit them to BREC for review. Except in emergency situations, no change to the protocol may be implemented until you have received written BREC approval for the change.

The committee will be notified of the above approval at its next meeting to be held on 08 July 2025.

Yours sincerely

[redacted]

Ms A Marimuthu
(for) Prof S Singh
Chair: Biomedical Research Ethics Committee

Biomedical Research Ethics Committee
Chair: Professor S Singh
UKZN Research Ethics Office Westville Campus, Govan Mbeki Building
Postal Address: Private Bag X54001, Durban 4000
Email: BREC@ukzn.ac.za
Website: https://research.ukzn.ac.za/research-office/ethics-overview/biomedical-research-ethics/
Founding Campuses: Edgewood Howard College Medical School Pietermaritzburg Westville

INSPIRING GREATNESS

Appendix IV – Current ethical approval letter for the FRESH cohort

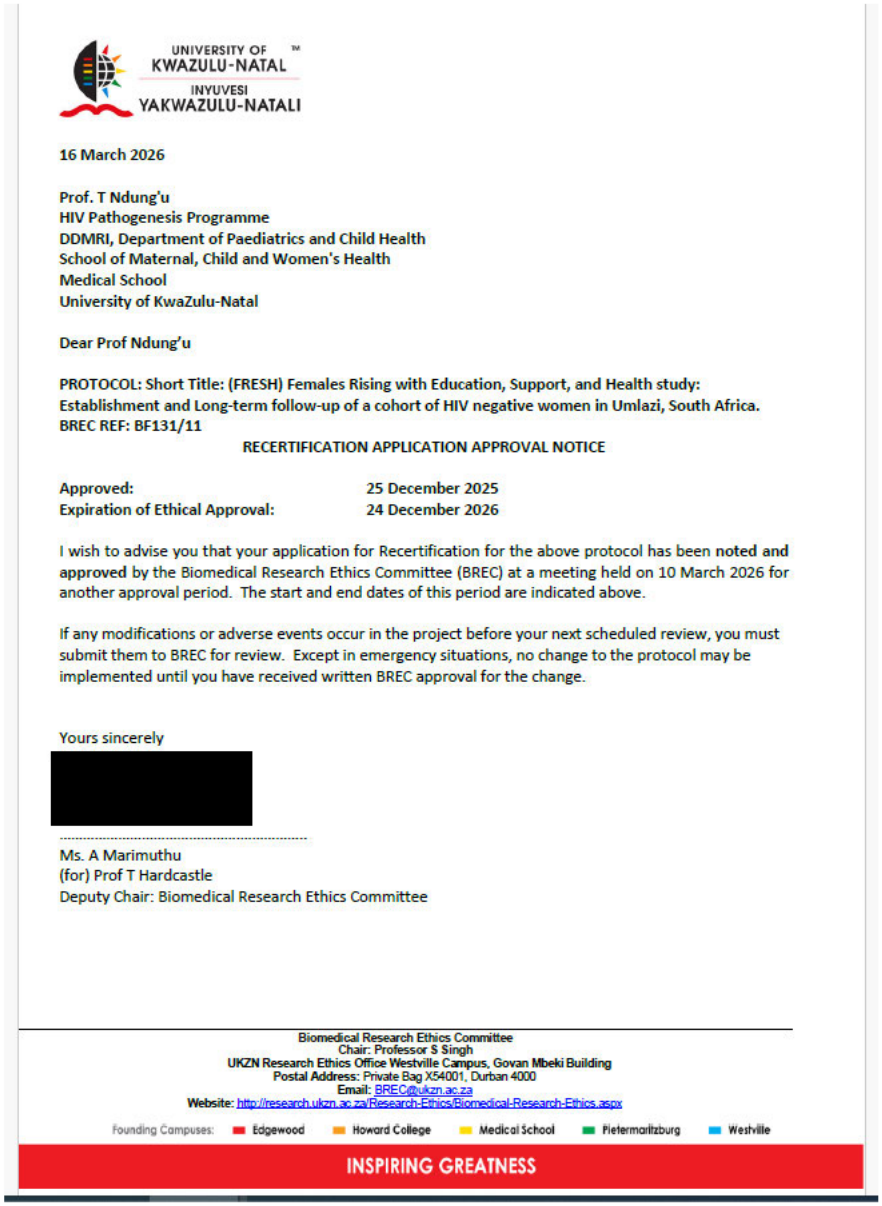

UNIVERSITY OF KWAZULU-NATAL
INYUVESI YAKWAZULU-NATALI

16 March 2026

Prof. T Ndung'u
HIV Pathogenesis Programme
DDMRI, Department of Paediatrics and Child Health
School of Maternal, Child and Women's Health
Medical School
University of KwaZulu-Natal

Dear Prof Ndung'u

PROTOCOL: Short Title: (FRESH) Females Rising with Education, Support, and Health study: Establishment and Long-term follow-up of a cohort of HIV negative women in Umlazi, South Africa.
BREC REF: BF131/11

RECERTIFICATION APPLICATION APPROVAL NOTICE

Approved: 25 December 2025
Expiration of Ethical Approval: 24 December 2026

I wish to advise you that your application for Recertification for the above protocol has been noted and approved by the Biomedical Research Ethics Committee (BREC) at a meeting held on 10 March 2026 for another approval period. The start and end dates of this period are indicated above.

If any modifications or adverse events occur in the project before your next scheduled review, you must submit them to BREC for review. Except in emergency situations, no change to the protocol may be implemented until you have received written BREC approval for the change.

Yours sincerely

[redacted]

Ms. A Marimuthu
(for) Prof T Hardcastle
Deputy Chair: Biomedical Research Ethics Committee

Biomedical Research Ethics Committee
Chair: Professor S Singh
UKZN Research Ethics Office Westville Campus, Govan Mbeki Building
Postal Address: Private Bag X54001, Durban 4000
Email: BREC@ukzn.ac.za
Website: http://research.ukzn.ac.za/Research-Ethics/Biomedical-Research-Ethics.aspx

Founding Campuses: Edgewood Howard College Medical School Pietermaritzburg Westville

INSPIRING GREATNESS

Appendix V – Ethical approval letter for the current study

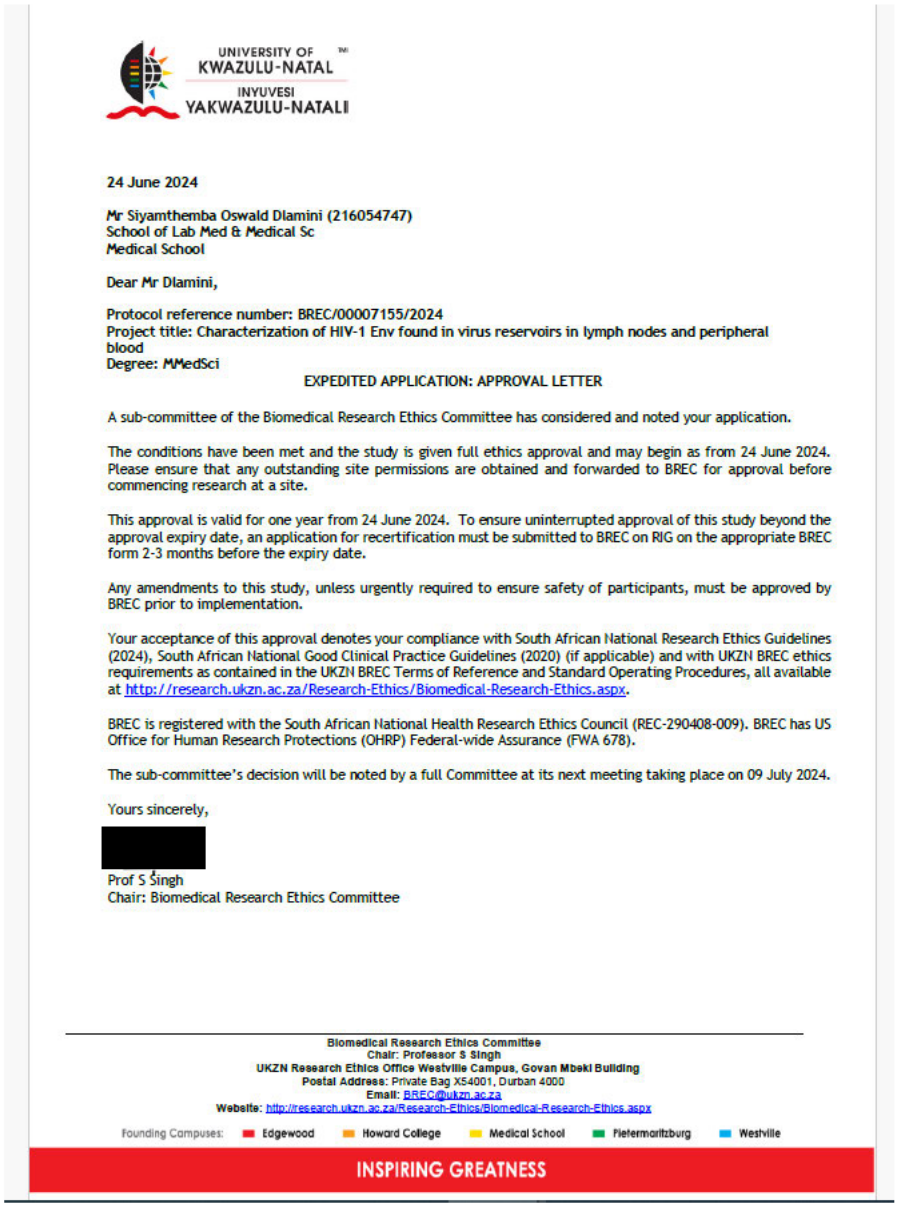

UNIVERSITY OF KWAZULU-NATAL
INYUVESI YAKWAZULU-NATALI

24 June 2024

Mr Siyamthemba Oswald Dlamini (216054747)
School of Lab Med & Medical Sc
Medical School

Dear Mr Dlamini,

Protocol reference number: BREC/00007155/2024
Project title: Characterization of HIV-1 Env found in virus reservoirs in lymph nodes and peripheral blood
Degree: MMedSci

EXPEDITED APPLICATION: APPROVAL LETTER

A sub-committee of the Biomedical Research Ethics Committee has considered and noted your application.

The conditions have been met and the study is given full ethics approval and may begin as from 24 June 2024. Please ensure that any outstanding site permissions are obtained and forwarded to BREC for approval before commencing research at a site.

This approval is valid for one year from 24 June 2024. To ensure uninterrupted approval of this study beyond the approval expiry date, an application for recertification must be submitted to BREC on RIG on the appropriate BREC form 2-3 months before the expiry date.

Any amendments to this study, unless urgently required to ensure safety of participants, must be approved by BREC prior to implementation.

Your acceptance of this approval denotes your compliance with South African National Research Ethics Guidelines (2024), South African National Good Clinical Practice Guidelines (2020) (if applicable) and with UKZN BREC ethics requirements as contained in the UKZN BREC Terms of Reference and Standard Operating Procedures, all available at http://research.ukzn.ac.za/Research-Ethics/Biomedical-Research-Ethics.aspx.

BREC is registered with the South African National Health Research Ethics Council (REC-290408-009). BREC has US Office for Human Research Protections (OHRP) Federal-wide Assurance (FWA 678).

The sub-committee's decision will be noted by a full Committee at its next meeting taking place on 09 July 2024.

Yours sincerely,

[redacted]

Prof S Singh
Chair: Biomedical Research Ethics Committee

Biomedical Research Ethics Committee
Chair: Professor S Singh
UKZN Research Ethics Office Westville Campus, Govan Mbeki Building
Postal Address: Private Bag X54001, Durban 4000
Email: BREC@ukzn.ac.za
Website: http://research.ukzn.ac.za/Research-Ethics/Biomedical-Research-Ethics.aspx

Founding Campuses: Edgewood Howard College Medical School Pietermaritzburg Westville

INSPIRING GREATNESS

References

1. Ndung'u, T., J.M. McCune, and S.G. Deeks, *Why and where an HIV cure is needed and how it might be achieved.* Nature, 2019. **576**(7787): p. 397-405.
2. Shaikh, K., et al., *Coronary artery plaque progression and cardiovascular risk scores in men with and without HIV-infection.* Aids, 2022. **36**(2): p. 215-224.
3. Hütter, G., et al., *Long-term control of HIV by CCR5 Delta32/Delta32 stem-cell transplantation.* N Engl J Med, 2009. **360**(7): p. 692-8.
4. Gupta, R.K., et al., *HIV-1 remission following CCR5Δ32/Δ32 haematopoietic stem-cell transplantation.* Nature, 2019. **568**(7751): p. 244-248.
5. Wright Jaclyn, K., et al., *Gag-Protease-Mediated Replication Capacity in HIV-1 Subtype C Chronic Infection: Associations with HLA Type and Clinical Parameters.* Journal of Virology, 2010. **84**(20): p. 10820-10831.
6. Engelman, A. and P. Cherepanov, *The structural biology of HIV-1: mechanistic and therapeutic insights.* Nature Reviews Microbiology, 2012. **10**(4): p. 279-290.
7. Gall, A., et al., *Complete Genome Sequence of the WHO International Standard for HIV-1 RNA Determined by Deep Sequencing.* Genome Announcements, 2014. **2**(1): p. 10.1128/genomea.01254-13.
8. Prabakaran, P., et al., *Structure and function of the HIV envelope glycoprotein as entry mediator, vaccine immunogen, and target for inhibitors.* Adv Pharmacol, 2007. **55**: p. 33-97.
9. Hu, W.S. and S.H. Hughes, *HIV-1 reverse transcription.* Cold Spring Harb Perspect Med, 2012. **2**(10).
10. Craigie, R. and F.D. Bushman, *HIV DNA integration.* Cold Spring Harb Perspect Med, 2012. **2**(7): p. a006890.
11. Karn, J. and C.M. Stoltzfus, *Transcriptional and posttranscriptional regulation of HIV-1 gene expression.* Cold Spring Harb Perspect Med, 2012. **2**(2): p. a006916.
12. Frankel, A.D. and J.A. Young, *HIV-1: fifteen proteins and an RNA.* Annu Rev Biochem, 1998. **67**: p. 1-25.
13. Freed, E.O., *HIV-1 assembly, release and maturation.* Nat Rev Microbiol, 2015. **13**(8): p. 484-96.
14. Sundquist, W.I. and H.G. Kräusslich, *HIV-1 assembly, budding, and maturation.* Cold Spring Harb Perspect Med, 2012. **2**(7): p. a006924.
15. Wilen, C.B., J.C. Tilton, and R.W. Doms, *HIV: cell binding and entry.* Cold Spring Harb Perspect Med, 2012. **2**(8).
16. Cohen, M.S., et al., *Acute HIV-1 Infection.* N Engl J Med, 2011. **364**(20): p. 1943-54.
17. Iwasaki, A., *Innate immune recognition of HIV-1.* Immunity, 2012. **37**(3): p. 389-98.
18. McMichael, A.J., et al., *The immune response during acute HIV-1 infection: clues for vaccine development.* Nat Rev Immunol, 2010. **10**(1): p. 11-23.
19. Goulder, P.J. and D.I. Watkins, *Impact of MHC class I diversity on immune control of immunodeficiency virus replication.* Nat Rev Immunol, 2008. **8**(8): p. 619-30.
20. Brenchley, J.M., et al., *Microbial translocation is a cause of systemic immune activation in chronic HIV infection.* Nat Med, 2006. **12**(12): p. 1365-71.
21. Masur, H., J.E. Kaplan, and K.K. Holmes, *Guidelines for preventing opportunistic infections among HIV-infected persons--2002. Recommendations of the U.S. Public Health Service and the Infectious Diseases Society of America.* Ann Intern Med, 2002. **137**(5 Pt 2): p. 435-78.
22. Siliciano, R.F. and W.C. Greene, *HIV latency.* Cold Spring Harb Perspect Med, 2011. **1**(1): p. a007096.
23. Chun, T.W., et al., *Presence of an inducible HIV-1 latent reservoir during highly active antiretroviral therapy.* Proc Natl Acad Sci U S A, 1997. **94**(24): p. 13193-7.
24. Archin, N.M., et al., *Administration of vorinostat disrupts HIV-1 latency in patients on antiretroviral therapy.* Nature, 2012. **487**(7408): p. 482-5.
25. Mbonye, U. and J. Karn, *Transcriptional control of HIV latency: cellular signaling pathways, epigenetics, happenstance and the hope for a cure.* Virology, 2014. **454-455**: p. 328-39.

26. Honeycutt, J.B., et al., *Macrophages sustain HIV replication in vivo independently of T cells.* J Clin Invest, 2016. **126**(4): p. 1353-66.
27. Estes, J.D., et al., *Defining total-body AIDS-virus burden with implications for curative strategies.* Nat Med, 2017. **23**(11): p. 1271-1276.
28. Maldarelli, F., et al., *HIV latency. Specific HIV integration sites are linked to clonal expansion and persistence of infected cells.* Science, 2014. **345**(6193): p. 179-83.
29. Banga, R. and M. Perreau, *The multifaceted nature of HIV tissue reservoirs.* Curr Opin HIV AIDS, 2024. **19**(3): p. 116-123.
30. Josefsson, L., et al., *The HIV-1 reservoir in eight patients on long-term suppressive antiretroviral therapy is stable with few genetic changes over time.* Proceedings of the National Academy of Sciences, 2013. **110**(51): p. E4987-E4996.
31. Cavrois, M., et al., *Human immunodeficiency virus fusion to dendritic cells declines as cells mature.* J Virol, 2006. **80**(4): p. 1992-9.
32. Churchill, M.J., et al., *Use of laser capture microdissection to detect integrated HIV-1 DNA in macrophages and astrocytes from autopsy brain tissues.* J Neurovirol, 2006. **12**(2): p. 146-52.
33. Wang, L.L., et al., *Revisiting astrocyte to neuron conversion with lineage tracing in vivo.* Cell, 2021. **184**(21): p. 5465-5481.e16.
34. Cohn, L.B., N. Chomont, and S.G. Deeks, *The Biology of the HIV-1 Latent Reservoir and Implications for Cure Strategies.* Cell Host Microbe, 2020. **27**(4): p. 519-530.
35. Banga, R., O. Munoz, and M. Perreau, *HIV persistence in lymph nodes.* Curr Opin HIV AIDS, 2021. **16**(4): p. 209-214.
36. Busman-Sahay, K., et al., *Eliminating HIV reservoirs for a cure: the issue is in the tissue.* Curr Opin HIV AIDS, 2021. **16**(4): p. 200-208.
37. Heesters, B.A., et al., *Follicular Dendritic Cells Retain Infectious HIV in Cycling Endosomes.* PLoS Pathog, 2015. **11**(12): p. e1005285.
38. Fukazawa, Y., et al., *B cell follicle sanctuary permits persistent productive simian immunodeficiency virus infection in elite controllers.* Nat Med, 2015. **21**(2): p. 132-9.
39. De Scheerder, M.A., et al., *HIV Rebound Is Predominantly Fueled by Genetically Identical Viral Expansions from Diverse Reservoirs.* Cell Host Microbe, 2019. **26**(3): p. 347-358.e7.
40. Immonen, T.T., et al., *No evidence for ongoing replication on ART in SIV-infected macaques.* Nat Commun, 2024. **15**(1): p. 5093.
41. Fletcher, C.V., et al., *Persistent HIV-1 replication is associated with lower antiretroviral drug concentrations in lymphatic tissues.* Proc Natl Acad Sci U S A, 2014. **111**(6): p. 2307-12.
42. Solis-Leal, A., et al., *Lymphoid tissues contribute to plasma viral clonotypes early after antiretroviral therapy interruption in SIV-infected rhesus macaques.* Sci Transl Med, 2023. **15**(726): p. eadi9867.
43. Gandhi, M., et al., *Does patient sex affect human immunodeficiency virus levels?* Clin Infect Dis, 2002. **35**(3): p. 313-22.
44. Scully, E.P., et al., *Sex-Based Differences in Human Immunodeficiency Virus Type 1 Reservoir Activity and Residual Immune Activation.* J Infect Dis, 2019. **219**(7): p. 1084-1094.
45. Das, B., et al., *Estrogen receptor-1 is a key regulator of HIV-1 latency that imparts gender-specific restrictions on the latent reservoir.* Proc Natl Acad Sci U S A, 2018. **115**(33): p. E7795-e7804.
46. Garcia-Broncano, P., et al., *Early antiretroviral therapy in neonates with HIV-1 infection restricts viral reservoir size and induces a distinct innate immune profile.* Sci Transl Med, 2019. **11**(520).
47. Dhummakupt, A., et al., *Differences in inducibility of the latent HIV reservoir in perinatal and adult infection.* JCI Insight, 2020. **5**(4).
48. Thome, J.J., et al., *Spatial map of human T cell compartmentalization and maintenance over decades of life.* Cell, 2014. **159**(4): p. 814-28.
49. Persaud, D., et al., *Influence of age at virologic control on peripheral blood human immunodeficiency virus reservoir size and serostatus in perinatally infected adolescents.* JAMA Pediatr, 2014. **168**(12): p. 1138-46.

50. Prodger, J.L., et al., *Reduced Frequency of Cells Latently Infected With Replication-Competent Human Immunodeficiency Virus-1 in Virally Suppressed Individuals Living in Rakai, Uganda.* Clin Infect Dis, 2017. **65**(8): p. 1308-1315.
51. Omondi, F.H., et al., *HIV Subtype and Nef-Mediated Immune Evasion Function Correlate with Viral Reservoir Size in Early-Treated Individuals.* J Virol, 2019. **93**(6).
52. Pache, L., et al., *BIRC2/cIAP1 Is a Negative Regulator of HIV-1 Transcription and Can Be Targeted by Smac Mimetics to Promote Reversal of Viral Latency.* Cell Host Microbe, 2015. **18**(3): p. 345-53.
53. Nixon, C.C., et al., *Systemic HIV and SIV latency reversal via non-canonical NF-κB signalling in vivo.* Nature, 2020. **578**(7793): p. 160-165.
54. Borducchi, E.N., et al., *Ad26/MVA therapeutic vaccination with TLR7 stimulation in SIV-infected rhesus monkeys.* Nature, 2016. **540**(7632): p. 284-287.
55. Schulz, W.A., C. Steinhoff, and A.R. Florl, *Methylation of endogenous human retroelements in health and disease.* Curr Top Microbiol Immunol, 2006. **310**: p. 211-50.
56. Mousseau, G., et al., *The Tat Inhibitor Didehydro-Cortistatin A Prevents HIV-1 Reactivation from Latency.* mBio, 2015. **6**(4): p. e00465.
57. Kessing, C.F., et al., *In Vivo Suppression of HIV Rebound by Didehydro-Cortistatin A, a "Block-and-Lock" Strategy for HIV-1 Treatment.* Cell Rep, 2017. **21**(3): p. 600-611.
58. Vandergeeten, C., et al., *Interleukin-7 promotes HIV persistence during antiretroviral therapy.* Blood, 2013. **121**(21): p. 4321-9.
59. Sok, D. and D.R. Burton, *Recent progress in broadly neutralizing antibodies to HIV.* Nat Immunol, 2018. **19**(11): p. 1179-1188.
60. Burton, D.R. and L. Hangartner, *Broadly Neutralizing Antibodies to HIV and Their Role in Vaccine Design.* Annu Rev Immunol, 2016. **34**: p. 635-59.
61. Kwong, P.D. and J.R. Mascola, *HIV-1 Vaccines Based on Antibody Identification, B Cell Ontogeny, and Epitope Structure.* Immunity, 2018. **48**(5): p. 855-871.
62. Bournazos, S., et al., *Broadly neutralizing anti-HIV-1 antibodies require Fc effector functions for in vivo activity.* Cell, 2014. **158**(6): p. 1243-1253.
63. Niessl, J., et al., *Combination anti-HIV-1 antibody therapy is associated with increased virus-specific T cell immunity.* Nat Med, 2020. **26**(2): p. 222-227.
64. Walsh, S.R. and M.S. Seaman, *Broadly Neutralizing Antibodies for HIV-1 Prevention.* Front Immunol, 2021. **12**: p. 712122.
65. Pancera, M., et al., *Structure of HIV-1 gp120 with gp41-interactive region reveals layered envelope architecture and basis of conformational mobility.* Proc Natl Acad Sci U S A, 2010. **107**(3): p. 1166-71.
66. Checkley, M.A., B.G. Luttge, and E.O. Freed, *HIV-1 envelope glycoprotein biosynthesis, trafficking, and incorporation.* J Mol Biol, 2011. **410**(4): p. 582-608.
67. Wang, Q., A. Finzi, and J. Sodroski, *The Conformational States of the HIV-1 Envelope Glycoproteins.* Trends Microbiol, 2020. **28**(8): p. 655-667.
68. Julien, J.P., et al., *Crystal structure of a soluble cleaved HIV-1 envelope trimer.* Science, 2013. **342**(6165): p. 1477-83.
69. Kwong, P.D., et al., *Structure of an HIV gp120 envelope glycoprotein in complex with the CD4 receptor and a neutralizing human antibody.* Nature, 1998. **393**(6686): p. 648-59.
70. Miyauchi, K., et al., *HIV enters cells via endocytosis and dynamin-dependent fusion with endosomes.* Cell, 2009. **137**(3): p. 433-44.
71. Harrison, S.C., *Viral membrane fusion.* Virology, 2015. **479-480**: p. 498-507.
72. Elalouf, A., H. Elalouf, and H. Maoz, *HIV-1 Entry Mechanisms: Protein-Host Receptor Interactions and Membrane Fusion Dynamics.* Front Biosci (Landmark Ed), 2025. **30**(10): p. 37412.
73. Ward, A.B. and I.A. Wilson, *The HIV-1 envelope glycoprotein structure: nailing down a moving target.* Immunol Rev, 2017. **275**(1): p. 21-32.
74. Wei, X., et al., *Antibody neutralization and escape by HIV-1.* Nature, 2003. **422**(6929): p. 307-12.
75. Schorcht, A., et al., *The Glycan Hole Area of HIV-1 Envelope Trimers Contributes Prominently to the Induction of Autologous Neutralization.* J Virol, 2022. **96**(1): p. e0155221.

76. Stewart-Jones, G.B., et al., *Trimeric HIV-1-Env Structures Define Glycan Shields from Clades A, B, and G.* Cell, 2016. **165**(4): p. 813-26.
77. Behrens, A.J., et al., *Composition and Antigenic Effects of Individual Glycan Sites of a Trimeric HIV-1 Envelope Glycoprotein.* Cell Rep, 2016. **14**(11): p. 2695-706.
78. Crispin, M., A.B. Ward, and I.A. Wilson, *Structure and Immune Recognition of the HIV Glycan Shield.* Annu Rev Biophys, 2018. **47**: p. 499-523.
79. Wibmer, C.K., et al., *Structure and Recognition of a Novel HIV-1 gp120-gp41 Interface Antibody that Caused MPER Exposure through Viral Escape.* PLoS Pathog, 2017. **13**(1): p. e1006074.
80. Munro, J.B., et al., *Conformational dynamics of single HIV-1 envelope trimers on the surface of native virions.* Science, 2014. **346**(6210): p. 759-63.
81. Moody, M.A., et al., *Strain-Specific V3 and CD4 Binding Site Autologous HIV-1 Neutralizing Antibodies Select Neutralization-Resistant Viruses.* Cell Host Microbe, 2015. **18**(3): p. 354-62.
82. Freund, N.T., et al., *Coexistence of potent HIV-1 broadly neutralizing antibodies and antibody-sensitive viruses in a viremic controller.* Sci Transl Med, 2017. **9**(373).
83. Blattner, C., et al., *Structural delineation of a quaternary, cleavage-dependent epitope at the gp41-gp120 interface on intact HIV-1 Env trimers.* Immunity, 2014. **40**(5): p. 669-80.
84. Scharf, L., et al., *Antibody 8ANC195 reveals a site of broad vulnerability on the HIV-1 envelope spike.* Cell Rep, 2014. **7**(3): p. 785-95.
85. Williams, L.D., et al., *Potent and broad HIV-neutralizing antibodies in memory B cells and plasma.* Sci Immunol, 2017. **2**(7).
86. Kong, L., et al., *Complete epitopes for vaccine design derived from a crystal structure of the broadly neutralizing antibodies PGT128 and 8ANC195 in complex with an HIV-1 Env trimer.* Acta Crystallogr D Biol Crystallogr, 2015. **71**(Pt 10): p. 2099-108.
87. Cardoso, R.M., et al., *Broadly neutralizing anti-HIV antibody 4E10 recognizes a helical conformation of a highly conserved fusion-associated motif in gp41.* Immunity, 2005. **22**(2): p. 163-73.
88. Walker, L.M., et al., *Broad and potent neutralizing antibodies from an African donor reveal a new HIV-1 vaccine target.* Science, 2009. **326**(5950): p. 285-9.
89. Julg, B. and D. Barouch, *Broadly neutralizing antibodies for HIV-1 prevention and therapy.* Semin Immunol, 2021. **51**: p. 101475.
90. Zhang, Z., et al., *Antiviral Therapy by HIV-1 Broadly Neutralizing and Inhibitory Antibodies.* Int J Mol Sci, 2016. **17**(11).
91. Stefic, K., et al., *Probing the compartmentalization of HIV-1 in the central nervous system through its neutralization properties.* PLoS One, 2017. **12**(8): p. e0181680.
92. Jeewanraj, N., et al., *Partial compartmentalisation of HIV-1 subtype C between lymph nodes, peripheral blood mononuclear cells and plasma.* Virology, 2023. **582**: p. 62-70.
93. Wang, C., et al., *Landscape of Human Immunodeficiency Virus Neutralization Susceptibilities Across Tissue Reservoirs.* Clin Infect Dis, 2022. **75**(8): p. 1342-1350.
94. McManus, W.R., et al., *HIV-1 in lymph nodes is maintained by cellular proliferation during antiretroviral therapy.* J Clin Invest, 2019. **129**(11): p. 4629-4642.
95. Ojwach, D., et al., *Limited Sequence Variation and Similar Phenotypic Characteristics of HIV-1 Subtype C Gag Variants Derived From the Reservoir and Pre-Therapy Plasma.* Frontiers in Virology, 2022. **Volume 2 - 2022**.
96. Mandizvo, T., et al., *Subtle Longitudinal Alterations in Env Sequence Potentiate Differences in Sensitivity to Broadly Neutralizing Antibodies following Acute HIV-1 Subtype C Infection.* J Virol, 2022. **96**(24): p. e0127022.
97. Archary, D., et al., *HIV-1 subtype C envelope characteristics associated with divergent rates of chronic disease progression.* Retrovirology, 2010. **7**: p. 92.
98. Cale, E.M., et al., *Virus-like Particles Identify an HIV V1V2 Apex-Binding Neutralizing Antibody that Lacks a Protruding Loop.* Immunity, 2017. **46**(5): p. 777-791.e10.
99. Doria-Rose, N.A., et al., *New Member of the V1V2-Directed CAP256-VRC26 Lineage That Shows Increased Breadth and Exceptional Potency.* J Virol, 2016. **90**(1): p. 76-91.
100. Lee, J.H., et al., *Antibodies to a conformational epitope on gp41 neutralize HIV-1 by destabilizing the Env spike.* Nat Commun, 2015. **6**: p. 8167.

101. Roark, R.S., et al., *Recapitulation of HIV-1 Env-antibody coevolution in macaques leading to neutralization breadth.* Science, 2021. **371**(6525).
102. Bricault, C.A., et al., *HIV-1 Neutralizing Antibody Signatures and Application to Epitope-Targeted Vaccine Design.* Cell Host Microbe, 2019. **25**(1): p. 59-72.e8.
103. Lee, J.H., et al., *A Broadly Neutralizing Antibody Targets the Dynamic HIV Envelope Trimer Apex via a Long, Rigidified, and Anionic β-Hairpin Structure.* Immunity, 2017. **46**(4): p. 690-702.
104. Gao, N., et al., *Development of Neutralization Breadth against Diverse HIV-1 by Increasing Ab-Ag Interface on V2.* Adv Sci (Weinh), 2022. **9**(15): p. e2200063.
105. Roark, R.S., et al., *Structural and genetic basis of HIV-1 envelope V2 apex recognition by rhesus broadly neutralizing antibodies.* J Exp Med, 2025. **222**(10).
106. Stanfield, R.L., et al., *Structural basis of broad HIV neutralization by a vaccine-induced cow antibody.* Sci Adv, 2020. **6**(22): p. eaba0468.
107. Huang, J., et al., *Identification of a CD4-Binding-Site Antibody to HIV that Evolved Near-Pan Neutralization Breadth.* Immunity, 2016. **45**(5): p. 1108-1121.
108. Yang, Z., et al., *Asymmetric opening of HIV-1 Env bound to CD4 and a coreceptor-mimicking antibody.* Nat Struct Mol Biol, 2019. **26**(12): p. 1167-1175.
109. Dingens, A.S., et al., *An Antigenic Atlas of HIV-1 Escape from Broadly Neutralizing Antibodies Distinguishes Functional and Structural Epitopes.* Immunity, 2019. **50**(2): p. 520-532.e3.
110. Falkowska, E., et al., *Broadly Neutralizing HIV Antibodies Define a Glycan-Dependent Epitope on the Prefusion Conformation of gp41 on Cleaved Envelope Trimers.* Immunity, 2014. **40**(5): p. 657-668.
111. Cottrell, C.A., et al., *Mapping the immunogenic landscape of near-native HIV-1 envelope trimers in non-human primates.* PLoS Pathog, 2020. **16**(8): p. e1008753.
112. Gao, F., et al., *Cooperation of B cell lineages in induction of HIV-1-broadly neutralizing antibodies.* Cell, 2014. **158**(3): p. 481-91.
113. Schommers, P., et al., *Restriction of HIV-1 Escape by a Highly Broad and Potent Neutralizing Antibody.* Cell, 2020. **180**(3): p. 471-489.e22.
114. Sok, D. and Dennis R. Burton, *HIV Broadly Neutralizing Antibodies: Taking Good Care Of The 98%.* Immunity, 2016. **45**(5): p. 958-960.
115. Pantophlet, R., *Antibody epitope exposure and neutralization of HIV-1.* Curr Pharm Des, 2010. **16**(33): p. 3729-43.
116. Peterhoff, D. and R. Wagner, *Guiding the long way to broad HIV neutralization.* Curr Opin HIV AIDS, 2017. **12**(3): p. 257-264.
117. Wu, X., et al., *Rational design of envelope identifies broadly neutralizing human monoclonal antibodies to HIV-1.* Science, 2010. **329**(5993): p. 856-61.
118. Ringe, R.P., et al., *Closing and Opening Holes in the Glycan Shield of HIV-1 Envelope Glycoprotein SOSIP Trimers Can Redirect the Neutralizing Antibody Response to the Newly Unmasked Epitopes.* J Virol, 2019. **93**(4).
119. Basu, S., et al., *Determination of Binding Affinity of Antibodies to HIV-1 Recombinant Envelope Glycoproteins, Pseudoviruses, Infectious Molecular Clones, and Cell-Expressed Trimeric gp160 Using Microscale Thermophoresis.* Cells, 2023. **13**(1).
120. Wu, Y., et al., *Structural basis for enhanced HIV-1 neutralization by a dimeric immunoglobulin G form of the glycan-recognizing antibody 2G12.* Cell Rep, 2013. **5**(5): p. 1443-55.
121. Kong, L., et al., *Supersite of immune vulnerability on the glycosylated face of HIV-1 envelope glycoprotein gp120.* Nat Struct Mol Biol, 2013. **20**(7): p. 796-803.
122. Dingens, A.S., et al., *Comprehensive Mapping of HIV-1 Escape from a Broadly Neutralizing Antibody.* Cell Host Microbe, 2017. **21**(6): p. 777-787.e4.
123. Ndlovu, B., et al., *Distinct neutralization sensitivity between adult and infant transmitted/founder HIV-1 subtype C viruses to broadly neutralizing monoclonal antibodies.* PLoS Pathog, 2025. **21**(6): p. e1013245.
124. Ndung'u, T., J.M. McCune, and S.G. Deeks, *Why and where an HIV cure is needed and how it might be achieved.* Nature, 2019. **576**(7787): p. 397-405.
125. Zhou, T., et al., *Structural Repertoire of HIV-1-Neutralizing Antibodies Targeting the CD4 Supersite in 14 Donors.* Cell, 2015. **161**(6): p. 1280-92.

126. Walker, L.M., et al., *Broad neutralization coverage of HIV by multiple highly potent antibodies.* Nature, 2011. **477**(7365): p. 466-70.
127. Andrabi, R., et al., *Identification of Common Features in Prototype Broadly Neutralizing Antibodies to HIV Envelope V2 Apex to Facilitate Vaccine Design.* Immunity, 2015. **43**(5): p. 959-73.
128. Caskey, M., et al., *Antibody 10-1074 suppresses viremia in HIV-1-infected individuals.* Nat Med, 2017. **23**(2): p. 185-191.
129. Li, M., et al., *Human immunodeficiency virus type 1 env clones from acute and early subtype B infections for standardized assessments of vaccine-elicited neutralizing antibodies.* J Virol, 2005. **79**(16): p. 10108-25.
130. Pritchard, L.K., et al., *Structural Constraints Determine the Glycosylation of HIV-1 Envelope Trimers.* Cell Rep, 2015. **11**(10): p. 1604-13.
131. Crooks, E.T., et al., *Enzyme digests eliminate nonfunctional Env from HIV-1 particle surfaces, leaving native Env trimers intact and viral infectivity unaffected.* J Virol, 2011. **85**(12): p. 5825-39.